Vanadium Complexes of the $N(CH_2CH_2S)_3^{3-}$ and $O(CH_2CH_2S)_2^{2-}$ Ligands with Coligands Relevant to Nitrogen Fixation Processes

Sian C. Davies,[†] David L. Hughes,[†] Zofia Janas,[‡] Lucjan B. Jerzykiewicz,[‡] Raymond L. Richards,[†] J. Roger Sanders,*[,†] James E. Silverston,[†] and Piotr Sobota[‡]

Nitrogen Fixation Laboratory, John Innes Centre, Colney Lane, Norwich NR4 7UH, U.K., and Faculty of Chemistry, University of Wroclaw, 14 F. Joliot-Curie Street, 50-383 Wroclaw, Poland

Received August 6, 1999

Vanadium(III) and vanadium(V) complexes derived from the tris(2-thiolatoethyl)amine ligand [$(NS_3)^{3-}$] and the bis(2-thiolatoethyl)ether ligand [$(OS_2)^{2-}$] have been synthesized with the aim of investigating the potential of these vanadium sites to bind dinitrogen and activate its reduction. Evidence is presented for the transient existence of {V(*NS*$_3$)(N$_2$)V(*NS*$_3$)}, and a series of mononuclear complexes containing hydrazine, hydrazide, imide, ammine, organic cyanide, and isocyanide ligands has been prepared and the chemistry of these complexes investigated. [V(*NS*$_3$)O] (**1**) reacts with an excess of N_2H_4 to give, probably via the intermediates {V(*NS*$_3$)(NNH$_2$)} (**2a**) and {V(*NS*$_3$)(N$_2$)V(*NS*$_3$)} (**3**), the V^{III} adduct [V(*NS*$_3$)(N_2H_4)] (**4**). If **1** is treated with 0.5 mol of N_2H_4, 0.5 mol of N_2 is evolved and green, insoluble [{V(*NS*$_3$)}$_n$] (**5**) results. Compound **4** is converted by disproportionation to [V(*NS*$_3$)-(NH_3)] (**6**), but **4** does not act as a catalyst for disproportionation of N_2H_4 nor does it act as a catalyst for its reduction by Zn/$HOC_6H_3Pr^i_2$-2,6. Compound **1** reacts with $NR^1_2NR^2_2$ (R^1 = H or $SiMe_3$; R^2_2 = Me_2, MePh, or HPh) to give the hydrazide complexes [V(*NS*$_3$)(NNR^2_2)] (R^2_2 = Me_2, **2b**; R^2_2 = MePh, **2c**; R^2_2 = HPh, **2d**), which are not protonated by anhydrous HBr nor are they reduced by Zn/$HOC_6H_3Pr^i_2$-2,6. Compound **2b** can also be prepared by reaction of [V(NNMe$_2$)(dipp)$_3$] (dipp = $OC_6H_3Pr^i_2$-2,6) with NS_3H_3. N_2H_4 is displaced quantitatively from **4** by anions to give the salts [NR^3_4][V(*NS*$_3$)X] (X = Cl, R^3 = Et, **7a**; X = Cl, R^3 = Ph, **7b**; X = Br, R^3 = Et, **7c**; X = N_3, R^3 = Bu^n, **7d**; X = N_3, R^3 = Et, **7e;** X = CN, R^3 = Et, **7f**). Compound **6** loses NH_3 thermally to give **5**, which can also be prepared from [VCl_3(THF)$_3$] and NS_3H_3/$LiBu^n$. Displacement of NH_3 from **6** by ligands L gives the adducts [V(*NS*$_3$)(L)] (L = MeCN, ν_{CN} 2264 cm^{-1}, **8a**; L = Bu^tNC, ν_{NC} 2173 cm^{-1}, **8b;** L = $C_6H_{11}NC$, ν_{NC} 2173 cm^{-1}, **8c**). Reaction of **4** with N_3SiMe_3 gives [V(*NS*$_3$)(NSiMe$_3$)] (**9**), which is converted to [V(*NS*$_3$)(NH)] (**10**) by hydrolysis and to [V(*NS*$_3$)(NCPh$_3$)] (**11**) by reaction with $ClCPh_3$. Compound **10** is converted into **1** by [NMe_4]OH and to [V(*NS*$_3$)NLi(THF)$_2$] (**12**) by $LiNPr^i$ in THF. A further range of imido complexes [V(*NS*$_3$)(NR^4)] (R^4 = C_6H_4Y-4, where Y = H (**13a**), OMe (**13b**), Me (**13c**), Cl (**13d**), Br (**13e**), NO_2 (**13f**); R^4 = C_6H_4Y-3, where Y = OMe (**13g**); Cl (**13h**); R^4 = $C_6H_3Y_2$-3,4, where Y = Me (**13i**); Cl (**13j**); R^4 = C_6H_{11} (**13k**)) has been prepared by reaction of **1** with R^4NCO. The precursor complex [V(*OS*$_2$)O(dipp)] (**14**) [OS_2^{2-} = $O(CH_2CH_2S)_2^{2-}$] has been prepared from [VO(OPr^i)$_3$], Hdipp, and OS_2H_2. It reacts with NH_2NMe_2 to give [V(*OS*$_2$)-(NNMe$_2$)(dipp)] (**15**) and with N_3SiMe_3 to give [V(*OS*$_2$)(NSiMe$_3$)(dipp)] (**16**). A second oxide precursor, formulated as [V(*OS*$_2$)$_{1.5}$O] (**17**), has also been obtained, and it reacts with $SiMe_3NHNMe_2$ to give [V(*OS*$_2$)(NNMe$_2$)(OSiMe$_3$)] (**18**). The X-ray crystal structures of the complexes **2b**, **2c**, **4**, **6**, **7a**, **8a**, **9**, **10**, **13d**, **14**, **15, 16**, and **18** have been determined, and the ^{51}V NMR and other spectroscopic parameters of the complexes are discussed in terms of electronic effects.

Introduction

The cofactor of molybdenum nitrogenase (FeMoco) is considered to be the site at which this enzyme converts nitrogen gas into ammonia.[1] FeMoco has been shown by X-ray crystallography to contain an $MoFe_7S_9$ cluster with the Mo atom ligated by one nitrogen, three sulfur, and two oxygen atoms,[2] and it is thought that the vanadium atom in the analogous vanadium nitrogenase[3] is in a similar environment, as is possibly one of the iron atoms in the third "iron-only" nitrogenase.[4] The chemistry of V, Mo, and Fe centers, which carry three sulfurs (plus other ligands) (MS_3 sites), is therefore of great importance in understanding the mode of action of these enzymes. In particular, if one or a number of these metals is directly involved in the reduction of N_2 to NH_3, the process might involve intermediate ligand species such as N_2H_m and NH_n (m = 0−4; n = 0−3)[5,6] bound at MS_3 sites.[7]

In terms of studies that might relate to the function of vanadium nitrogenase, while it has been demonstrated that S_3-ligated vanadium in cluster anions such as $[Fe_3S_4X_3V(DMF)_3]^-$

[†] John Innes Centre.
[‡] University of Wroclaw.

(1) Evans, D. J.; Henderson, R. A.; Smith, B. E. In *Bioinorganic Catalysis*, 2nd ed.; Reedjik, J., Bouwman, E., Eds.; Marcel Decker, Inc.: New York, 1999; Chapter 7.
(2) Rees, D. C.; Chan, M. K.; Kim, J. *Adv. Inorg. Chem.* **1993**, *40*, 89.
(3) Eady, R. R. *Chem. Rev.* **1996**, *96*, 3013 and references therein.
(4) Pau R. N. In *Biology and Biochemistry of Nitrogen Fixation*; Dilworth, M. J., Glenn, A. R., Eds.; Elsevier: Oxford, 1991; p 37.
(5) Henderson, R. A.; Leigh, G. J.; Pickett, C. J. *Adv. Inorg. Chem. Radiochem.* **1984**, *27*, 197.
(6) Galindo, A.; Hills, A.; Hughes, D. L.; Hughes, M.; Mason, J.; Richards, R. L. *J. Chem. Soc., Dalton Trans.* **1990**, 283.
(7) Richards, R. L. *Coord Chem. Rev.* **1996**, *154*, 83. Hidai, M.; Mizobe, Y. *Chem. Rev.* **1995**, *95*, 1115.

10.1021/ic9909476 CCC: $19.00
Published on Web 07/21/2000

Table 1. Selected Bond Dimensions in the Vanadium Complexes $[V^{III}(NS_3)Z^1]$, $[V^{V}(NS_3)Z^2]$, and $[V^{V}(OS_2)Z^3]$[a]

Z	V−N(NS_3)	mean V−S	mean N−V−S in NS_3 ligand	Z, V−Z	other dimensions in the Z ligand
				$[V^{III}(NS_3)Z^1]$	
NCMe, **8a**	2.147(2)	2.287(2)	86.3(4)	N, 2.097(2)	N(2)−C(7) 1.126(3); C(7)−C(8) 1.451(4); V−N(2)−C(7) 170.9(2);N(2)−C(7)−C(8) 177.2(3)
NH_3, **6**	2.155(8)	2.290(6)	86.1(2)	N, 2.154(7)	N(5)−H(5a) 0.92(3); N(5)−H(5b) 0.91(4); N(5)−H(5c) 0.92(4); N(5)···S(1′) 3.415(9); N(5)···S(3″) 3.670(9); N(5)···S(2″) 3.499(9)
NH_2NH_2, **4**, mol. 1	2.180(9)	2.306(4)	85.2(6)	N, 2.135(10)	N(15)−N(16) 1.48(2); V−N(15)−N(16) 111.7(8)
mol. 2	2.154(9)	2.296(7)	86.2(2)	N, 2.157(10)	N(25)−N(26) 1.46(2); V−N(25)−N(26) 115.3(7)
Cl,[b] **7a**	2.183(3)	2.304(1)	84.7(1)	Cl, 2.369(1)	
				$[V^{V}(NS_3)Z^2]$	
$NNMe_2$, **2b**	2.214(3)	2.263(3)	84.4(3)	N, 1.681(3)	N(2)−N(3) 1.305(5); V−N(2)−N(3) 173.9(4); N(3)−C(7) 1.40(2); N(3)−C(8) 1.50(2); N(2)−N(3)−C(7) 118.9(11); N(2)−N(3)−C(8) 115.3(12); C(7)−N(3)−C(8) 118.4(5)
NNMePh, **2c**	2.218(2)	2.265(2)	84.4(3)	N, 1.682(2)	N(2)−N(3) 1.310(3); V−N(2)−N(3) 177.8(2); N(3)−C(7) 1.459(3); N(3)−C(8)1.400(3); N(2)−N(3)−C(7) 117.1(2); N(2)−N(3)−C(8) 120.3(2); C(7)−N(3)−C(8) 122.6(2)
NC_6H_4Cl-4, **13d**	2.228(2)	2.251(3)	84.4(4)	N, 1.670(2)	N(5)−C(51) 1.379(3); V−N(5)−C(51) 171.0(2)
NH, **10**	2.234(2)	2.253(1)	83.8(3)	N, 1.638(3)	N(5)−H(5) 0.80(4); V−N(5)−H(5) 179(3); H(5)···S(1′) 2.62(4); N(5)−H(5)···S(1′) 158(4); N(5)···S(1′) 3.367(3)
$NSiMe_3$, **9**, str 1	2.271(6)	2.255(4)	83.6(4)	N, 1.647(6)	N(2)−Si 1.766(6); V−N(2)−Si 163.9(5)
str 2	2.263(5)	2.255(2)	83.7(5)	N, 1.642(5)	N(5)−Si(5) 1.786(5); V−N(5)−Si(5) 163.2(3)
O, **1** [16]	2.291(6)	2.246(2)	83.2(2)	O, 1.578(6)	

$[V^{V}(OS_2)Z^3(dipp)]$

Z^3	V−O(OS_2)	mean V−S	mean O−V−S in (OS_2) ligand	Z, V−Z	V−O_{eq}, O(2)	V−O(2)−C(11)	other dimensions in the Z ligand
$NNMe_2$,[c] **18**	2.148(2)	2.269(6)	81.8(6)	N, 1.678(2)	1.798(2)	*c*	N(1)−N(2) 1.300(3); V−N(1)−N(2) 164.6(2)
$NNMe_2$, **15**	2.165(2)	2.274(1)	81.9(5)	N, 1.675(3)	1.803(2)	134.1(2)	N(1)−N(2) 1.296(4); V−N(1)−N(2) 174.1(3)
$NSiMe_3$, **16**	2.210(4)	2.259(3)	81.4(7)	N, 1.635(5)	1.808(3)	129.8(3)	N−Si 1.747(5); V−N−Si 174.1(3)
O, **14**	2.225(2)	2.253(1)	80.2(3)	O, 1.573(2)	1.785(2)	134.1(2)	

[a] Bond lengths are in Ångstroms, angles in degrees. Atom labels may be found in the figures. Estimated standard deviations or standard deviations of mean values, are in parentheses. [b] In the anion $[V(NS_3)Cl]^-$. [c] Complex **18** is $[V^{V}(OS_2)(NNMe_2)(OSiMe_3)]$; the V−O(2)−Si angle is 139.3(1)°.

(X = Cl, Br, or I) binds hydrazine and catalyzes its reduction[8] and while hydrazines[9] and imides[10] have been shown to bind at mononuclear, thiolate-ligated vanadium, generally very little chemistry of reduced nitrogen species at vanadium in a sulfur-donor environment has been reported. To help redress this deficiency, we decided to use the ligands $N(CH_2CH_2S)_3^{3-}$ $[NS_3]^{3-}$ and $O(CH_2CH_2S)_2^{2-}$ $[OS_2]^{2-}$ to generate a range of complexes of N_2H_m, NH_n and related ligands at VNS_3 and VOS_2 sites. We aim to relate the nitrogen chemistry of these sulfur-ligated sites to that of analogous Mo and Fe sites[11] and also to that of other vanadium sites where dinitrogen is bound, e.g., in such compounds as $[(Pr^i_2N)_3V(\mu\text{-}N_2)V(Pr^i_2N)_3]$[12] and $[V(N_2)_2(dppe)_2]^-$,[13] and more generally to that of metallic sites at which dinitrogen is reduced to ammonia via an established series of mononuclear intermediate species, particularly hydrazide and imide complexes, e.g., in $[MoCl(NNH_2)(dppe)_2]^+$ and $[MoCl(NH)(dppe)_2]^+$ (dppe = $Ph_2PCH_2CH_2PPh_2$).[14,15]

By this means we aimed to gain knowledge of the potential of these vanadium−sulfur sites to bind dinitrogen and activate its reduction. The outcome of this vanadium work, some of which has been reported in a preliminary form,[11] is described below.

Results and Discussion

In the following discussion of the compounds that we have made, selected bond dimensions for all structurally characterized compounds are in Table 1 and full crystallographic details are in Tables 2 and 3.

Hydrazine and Hydrazide Complexes of the NS_3^{3-} Ligand. Treatment of $[VO(NS_3)]$[16] (**1**) with 4 equiv of anhydrous hydrazine in acetonitrile removes the oxide ligand to give, via the intermediates **2a** and **3** discussed below, an almost quantitative yield of the complex $[V(NS_3)(NH_2NH_2)]$ (**4**) as a poorly soluble yellow powder. Although crystals of **4** for an X-ray study were obtained, intensity data for **4** proved to be very difficult

(8) Malinak, S. M.; Demadis, K. D.; Coucouvanis, D. *J. Am. Chem. Soc.* **1995**, *117*, 3126.
(9) Le Floc'h, C.; Henderson, R. A.; Hitchcock, P. B.; Hughes, D. L.; Janas, Z.; Richards, R. L.; Sobota, P.; Szafert, S. *J. Chem. Soc., Dalton Trans.* **1996**, 2755. Henderson, R. A.; Janas, Z.; Richards, R. L.; Sobota, P. Unpublished results.
(10) Preuss, F.; Noichel, H.; Kaub, J. *Z. Naturforsch.* **1986**, *41b*, 1085.
(11) Davies, S. C.; Hughes, D. L.; Janas, Z.; Jerzykiewicz, L.; Richards, R. L.; Sanders, J. R.; Sobota, P. *J. Chem. Soc., Chem. Commun.* **1997**, 1261. Davies, S. C.; Hughes, D. L.; Richards, R. L.; Sanders, J. R. *J. Chem. Soc., Chem. Commun.* **1998**, 2699.
(12) Song, J.-I.; Berno, P.; Gambarotta, S. *J. Am. Chem. Soc.* **1994**, *116*, 6927.
(13) Rehder, D.; Woitha, C.; Priebsch, W.; Gailus, H. *J. Chem. Soc., Chem. Commun.* **1992**, 364.
(14) Chatt, J.; Heath, G. A.; Richards, R. L. *J. Chem. Soc., Dalton Trans.* **1974**, 2074.
(15) Chatt, J.; Dilworth, J. R. *J. Indian Chem. Soc.* **1977**, *54*, 13.

Table 2. Crystallographic Data for the Complexes [V(NS_3)Z][a]

compound	**2b**	**2c**	**4**	**6**	**7a**	**8a**	**9**, str 1	**9**, str 2	**10**	**13d**
Z	$NNMe_2$	NNMePh	NH_2NH_2	NH_3	Cl	NCMe	$NSiMe_3$	$NSiMe_3$	NH	NC_6H_4Cl-4
elemental formula	$C_8H_{18}N_3S_3V$	$C_{13}H_{20}N_3S_3V$	$C_6H_{16}N_3S_3V$	$C_6H_{15}N_2S_3V$	$C_8H_{20}N,C_6H_{12}ClNS_3V$	$C_8H_{15}N_2S_3V$	$C_9H_{21}N_2S_3SiV$	$C_9H_{21}N_2S_3SiV$	$C_6H_{13}N_2S_3V$	$C_{12}H_{16}ClN_2S_3V$
mol wt	303.4	365.4	277.3	262.3	411.0	286.3	332.5	332.5	260.3	370.8
crystal system	monoclinic	monoclinic	monoclinic	orthorhombic	orthorhombic	orthorhombic	monoclinic	monoclinic	triclinic	monoclinic
space group (no.)	$P2_1$ (4)	$P2_1/c$ (14)	$P2_1/n$ (≈14)[b]	$P2_12_12_1$ (19)	*Pbcm* (57)	*Pbca* (61)	$P2_1/c$ (14)	$P2_1/c$ (14)	P-1 (2)	$P2_1/a$ (≈14)
a (Å)	7.494(1)	12.713(4)	8.1566(8)	8.0612(6)	8.773(2)	11.787(2)	11.141(2)	11.1558(12)	7.4103(7)	13.5753(11)
b (Å)	11.649(2)	8.570(3)	13.584(2)	16.6065(13)	14.345(4)	12.090(3)	12.035(2)	12.040(11)	7.6619(9)	16.300(2)
c (Å)	7.584(1)	15.225(3)	21.264(17)	8.5004(12)	15.934(3)	17.576(4)	12.260(3)	12.2720(15)	10.5983(13)	7.4990(7)
α (deg)									86.359(9)	
β (deg)	92.03(1)	101.68(3)	100.32(4)				109.55(3)	109.545(9)	74.676(9)	102.258(7)
γ (deg)									65.116(9)	
V (Å^3)	661.5(2)	1624.4(8)	2318(2)	1137.9(2)	2005.3(8)	2504.7(9)	1549.1(5)	1553.4(3)	525.7(1)	1621.6(3)
no. formula units/cell, *Z*	2	4	8	4	4	8	4	4	2	4
ρ (g cm^{-3})	1.523	1.494	1.589	1.531	1.361	1.519	1.426	1.42	1.65	1.519
F(000)	316	760	1152	544	872	1184	696	696	268	760
μ(Mo Kα) (cm^{-1})	12.0	9.9	13.6	13.3	9.4	12.6	11.0	11.0	14.9	11.5
crystal color, shape	red, rectangular prisms	dark-red cubes	pale olive-green square prisms	yellow, translucent plates	red blocks	red cubes	orange square prisms	orange square prisms	brown-red triangular plates	deep-red blocks
crystal size (mm)	0.5 × 0.3 × 0.2	0.4 × 0.3 × 0.1	0.19 × 0.29 × 0.36	0.41 × 0.08 × 0.05	0.7 × 0.5 × 0.4	0.4 × 0.4 × 0.4	0.35 × 0.3 × 0.2	0.40 × 0.10 × 0 07	0.52 × 0.24 × 0.01	0.31 × 0.21 × 0.45
crystal mounting	in a glass capillary under N_2	in a glass capillary under N_2	on a glass fiber, sealed with epoxy resin	on a glass fiber	in a glass capillary, under N_2	in a glass capillary under N_2	in a glass capillary under N_2	on a glass fiber, sealed with epoxy resin	on a glass fiber, sealed with epoxy resin	on a glass fiber
θ for centered reflections (deg)	8.5−13	8.5−13	10−11	10−11	8−13	7.5−14	7−14	10−11	8−11	10−11
θ_{max} for data collection (deg)	25	25	25	25	25	25.1	25	20	25	25
h, *k*, *l* range	0/8, 0/13, −9/9	0/15, 0/10, −18/17	−9/9, −1/16, −1/25	−1/9, −1/19, −1/10	0/10, 0/17, 0/18	0/14, 0/14, −20/20	0/13, 0/14, −14/13	−10/10, 0/11, 0/11	−8/8, −9/9, 0/12	−16/16, −1/19, −1/8
cryst degradation (% overall)	0	0	9.7	1.0	6.5	0	15	0	4.7	3.3
transm coeff	not applied	not applied	0.96−1.0	0.81−0.81	not applied	as for sphere	not applied	0.96−1.0	0.98−0.99	0.87−0.99
total no. reflns measd (not including absences)	1749	2461	4382	1631	2057	3715	1522	1646	1952	3065
BAYES correction applied	no	no	yes	yes	yes	no	no	yes	yes	yes
R_{int} for equivalents	0.010	0.021	0.047	0.032	−	0.112	0.030	0.040	0.019	0.010
total no. of unique reflections	1218	2398	4028	1175	1846	1964	1453	1452	1841	2838
no. obsd reflections ($I > 2\sigma_I$)	1118	2186	2368	729	1357	1795	1372	832	1451	2375
structure determination	direct methods	direct methods	direct methods	automated Patterson	direct methods	direct methods	direct methods	automated Patterson	automated Patterson	direct methods
final R_1, wR_2	0.031, 0.087	0.039, 0.092	0.074, 0.237	0.085, 0.093	0.053, 0.118	0.037, 0.086	0.055, 0.145	0.102, 0.084	0.044, 0.083	0.035, 0.075
no. reflections used	1118 (with $I > 2\sigma_I$)	2398 (all data)	2368 (with $I > 2\sigma_I$)	1170 (all but 5)	1846 (all data)	1964 (all data)	1453 (all data)	1452 (all data)	1841 (all data)	2838 (all data)
no. parameters refined	154	212	376	169	182	128	145	166	189	185
R_1 for the obsd reflns	(0.031)	0.034	(0.074)	0.049	0.035	0.031	0.048	0.040	0.031	0.028
goodness-of-fit, *S* (on F^2)	1.20	1.10	0.85	1.06	1.11	1.12	1.15	1.04	1.05	1.08
reflns weighted, *w*	$\{\sigma^2(F_o^2) + (0.046P)^2 + 0.56P\}^{-1}$	$\{\sigma^2(F_o^2) + (0.062P)^2 + 0.48P\}^{-1}$	$\{\sigma^2(F_o^2) + (0.1P)^2\}^{-1}$	$\sigma^{-2}(F_o^2)$	$\{\sigma^2(F_o^2) + (0.073P)^2 + 0.56P\}^{-1}$	$\{\sigma^2(F_o^2) + (0.048P)^2 + 1.37P\}^{-1}$	$\{\sigma^2(F_o^2) + (0.088P)^2 + 3.80P\}^{-1}$	$\{\sigma^2(F_o^2) + (0.011P)^2\}^{-1}$	$\{\sigma^2(F_o^2) + (0.038P)^2 + 0.11P\}^{-1}$	$\{\sigma^{-2}(F_o^2) + (0.013P)^2 + 0.71P\}^{-1}$
final difference map										
highest peaks (e Å^{-3})	0.36	0.48	0.55	0.35	0.32	0.50	0.60	0.37	0.35	0.23
location	in the thiolate ligand.	V atom	close to V centers	near ammine N atom	in anion, near Cl	C3 atom	S1 atom	close to a S atom	close to a S atom	close to S or Cl atoms

[a] *λ*(Mo Kα) for all analyses is 0.710 69 Å. [b] Composite cell of a twinned crystal.

Table 3. Crystallographic Data for the Complexes [V(OS_2)Z(dipp)][a]

compound	**14**	**15**	**16**	**18**
Z	O	$NNMe_2$	$NSiMe_3$	$NNMe_2$[b]
elemental formula	$C_{16}H_{25}O_3S_2V$	$C_{18}H_{31}N_2O_2S_2V$	$C_{19}H_{34}NO_2S_2SiV$	$C_9H_{23}N_2O_2S_2SiV$
mol wt	380.4	422.5	451.6	334.4
crystal system	monoclinic	monoclinic	triclinic	monoclinic
space group (no.)	$P2_1/n$ (≈14)	$C2/c$ (15)	P-1 (2)	$P2_1/c$ (14)
a (Å)	10.569(2)	19.151(5)	9.646(2)	15.223(5)
b (Å)	14.996(3)	7.606(4)	10.103(2)	12.207(4)
c (Å)	11.896(3)	31.258(9)	15.001(3)	9.091(4)
α (deg)			91.06(3)	
β (deg)	92.22(3)	100.26(5)	102.12(3)	93.53(4)
γ (deg)			118.16(3)	
V (Å^3)	1884.0(7)	4480(3)	1248.4(4)	1686.1(11)
no. formula units/cell, Z	4	8	2	4
ρ (g cm^{-3})	1.341	1.253	1.201	1.317
F(000)	800	1792	480	704
μ(Mo Kα) (cm^{-1})	7.6	6.4	6.2	9.0
crystal color, shape	red-orange cubes	red cubes	violet-red blocks	orange prisms
crystal size (mm.)	0.6 × 0.4 × 0.2	0.5 × 0.3 × 0.3	0.9 × 0.5 × 0.3	0.4 × 0.3 × 0.3
crystal mounting	in a glass capillary under N_2	in a glass capillary under N_2	in a glass capillary under N_2	in a glass capillary under N_2
θ for centered reflns (deg)	7.5−13	7.5−14	8−15	7.5−15
θ_{max} for data collection (deg)	25	30	25	25
h, k, l range	0/12, 0/17, −14/14	0/22, 0/10, −43/42	−9/0, −10/10, −17/17	−18/18, −14/0, 0/10
cryst degradation (% overall)	0	0	21.3	0
transm coeff	not applied	not applied	not applied	not applied
total no. reflns measd (not including absences)	2881	3652	2746	2434
BAYES correction applied	no	no	no	no
R_{int} for equivalents	0.007	0.073	0.021	0.013
total no. unique reflns	2722	3559	2541	2335
no. obsd reflns ($I > 2\sigma_I$)	2388	3047	2236	2053
structure determination	direct methods	direct methods	direct methods	direct methods
final R_1, wR_2	0.043, 0.098	0.058, 0.150	0.060, 0.172	0.039, 0.088
no. reflns used	2722 (all data)	3559 (all data)	2541 (all data)	2335 (all data)
no. parameters refined	199	232	242	159
R_1 for the obsd reflns	0.034	0.046	0.052	0.030
goodness-of-fit, S (on F^2)	1.08	1.07	1.12	1.10
reflns weighted, w	$\{\sigma^2(F_o^2) + (0.046P)^2 + 1.16P\}^{-1}$	$\{\sigma^2(F_o^2) + (0.098P)^2 + 5.84P\}^{-1}$	$\{\sigma^2(F_o^2) + (0.115P)^2 + 1.18P\}^{-1}$	$\{\sigma^2(F_o^2) + (0.047P)^2 + 0.75P\}^{-1}$
final difference map				
highest peaks (e Å^{-3})	0.47	0.73	0.62	0.42
location	S2 atom	C1 atom	V atom	N atom

[a] λ(Mo Kα) for all analyses is 0.710 69 Å. [b] Complex **18** is [V(OS_2)($NNMe_2$)($OSiMe_3$)].

to measure because all the crystals that we examined were twinned. Nevertheless, the solution of the structure showed clearly defined binding of the hydrazine molecule to vanadium (see Experimental Section).

Each twin (in the composite twinned cell) has two independent molecules. We shall describe only the structure of the major twin; the description of the minor twin is, of course, exactly the same, but the results are much less precise. The two independent molecules are virtually identical (Figure 1) with the same geometries and same dimensions. The V(NS_3) moiety is very similar to that found in the series of more accurately determined structures described below, with dimensions collated in Table 1. The hydrazine ligand in each molecule is end-on to the metal and bent at the ligating nitrogen with V−N−N angles of 111.7(8) and 115.3(7)°. These angles are in the range of those seen in related hydrazine complexes of vanadium(III), e.g., 121.05(5) and 122.7(4)° in [V($OC_6H_3Pr^i_2$-2,6)$_3$(NH_2NMe_2)$_2$].[9] The V−N and N−N distances, mean values of 2.146(11) and 1.469(11) Å, respectively, are both of single bonds.[9] Hydrogen atoms were not located in the hydrazine ligands, but their positions might be inferred from hydrogen bonding contacts. The molecules are linked in paired chains parallel to the a axis in the crystal by N−H···N hydrogen bonds, with additional N−H···S bonds within the chains. Contacts between chains are at normal van der Waals distances. The physical properties of **4** are presented in Experimental Section.

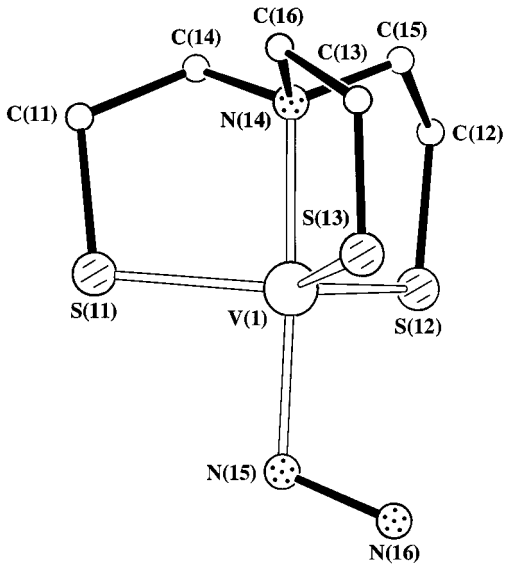

Figure 1. View of a molecule of [V(NS_3)(NH_2NH_2)], **4**. In the composite cell of the twinned crystal examined, there were two virtually identical, independent molecules (one shown here, with its atom numbering scheme) of the major twin plus two from the minor twin.

Scheme 1

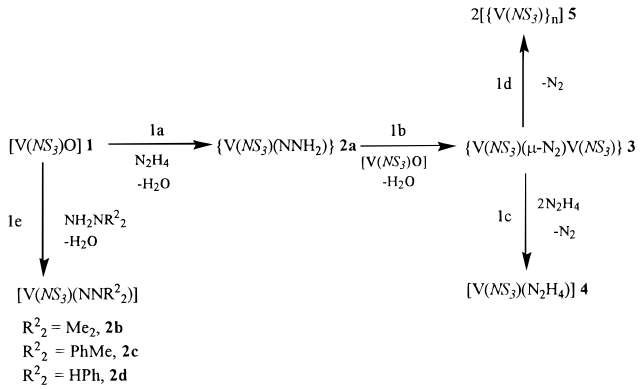

The formation of **4** might involve an intermediate dinitrogen complex $\{V(NS_3)(N_2)V(NS_3)\}$ (**3**) formed via a hydrazide intermediate $\{V(NS_3)(NNH_2)\}$ (**2a**) as shown in Scheme 1. Although the evidence for this reaction sequence is mainly circumstantial, we feel that it is a reasonable proposal for the following reasons. First, the overall stoichiometry of steps 1a → 1b → 1c has been established quantitatively (see Experimental Section). Second, when the reaction is carried out with only one hydrazine per two vanadiums (Scheme 1; 1a → 1b → 1d), an intermediate is observed that rapidly evolves 1 mol of N_2 to give 2 mol of $\{V(NS_3)\}$ (**5**). We have not been able to isolate this intermediate (**3**) in a characterizable form even at low temperature, but its formulation as $\{V(NS_3)(N_2)V(NS_3)\}$ appears reasonable in view of the products quantitatively derived from it and the fact that stable, linear vanadium(III) dinitrogen-bridged complexes are well-known, although with coligands other than sulfur.[12,17] The proposal of the hydrazide intermediate precursor to this bridged dinitrogen intermediate, $\{V(NS_3)(NNH_2)\}$ (**2a**), (step 1a in Scheme 1), follows because treatment of **1** with substituted hydrazines, $NR^1{}_2NR^2{}_2$ (R^1 = H or $SiMe_3$; $R^2{}_2$ = Me_2, MePh, or HPh), gives the diamagnetic hydrazide complexes $[V(NS_3)(NNR^2{}_2)]$ (**2b**−**d**), (step 1e of Scheme 1), which can be regarded as stabilized analogues of **2a** that cannot undergo step 1b in Scheme 1. Compound **2b** has also been prepared by reaction of $[V(OC_6H_3Pr^i{}_2\text{-}2,6)_3(NNMe_2)]$[18] with NS_3H_3 [reaction 1]. NMR and other physical properties of these

$$[V(OC_6H_3Pr^i{}_2\text{-}2,6)_3(NNMe_2)] + NS_3H_3 \xrightarrow{\text{hexanes}} [V(NS_3)(NNMe_2)]\ (\mathbf{2b}) + 3HOC_6H_3Pr^i{}_2\text{-}2,6 \quad (1)$$

complexes are listed in Experimental Section; ^{51}V NMR data are also discussed separately in the appropriate section below.

The structure of $[V(NS_3)(NNMe_2)]$ (**2b**) is very similar to that shown in Figure 1, and that of $[V(NS_3)(NNMePh)]$ (**2c**) is shown in Figure 2. Selected bond distances and angles are in Table 1. As far as we are aware, these are the first hydrazide complexes of vanadium with sulfur-donor coligands to be structurally characterized. In both compounds the geometry about the vanadium is trigonal bipyramidal with the S atoms in the equatorial positions and the N−V−N system almost linear.

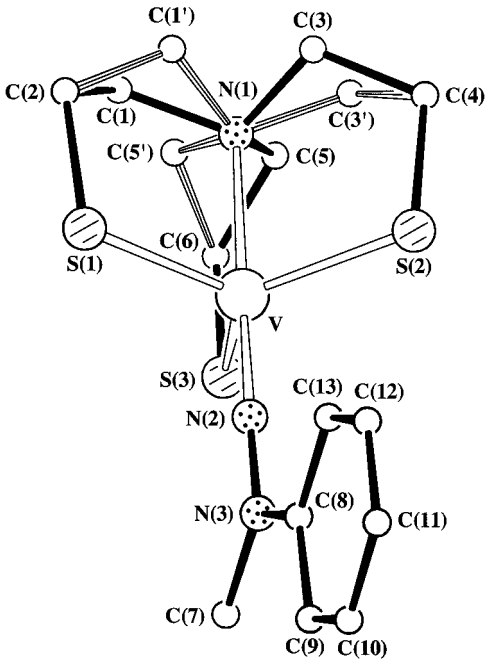

Figure 2. Molecule of the hydrazido(2-) complex $[V(NS_3)(NNMePh)]$ (**2c**), showing the alternative conformations of the NS_3 ligand.

This geometry is essentially maintained throughout the range of complexes of the $[NS_3]^{3-}$ ligand whose structures we present in this paper, and this allows us to compare the trans influence of ligands and other features at the $V(NS_3)$ site as are discussed below.

The N−N distance of the hydrazide ligands [1.305(5) Å in **2b** and 1.310(3) Å in **2c**] are in the range generally found[5,14,18,19] in hydrazide complexes of the early transition metals and in the only other structurally characterized hydrazide complexes of vanadium, $[V(C_5H_5)_2\{NN(SiMe_3)_2\}]$ [1.369(9) Å],[20] the anion $[VCl_2(NH_2NMePh)_2(NNMePh)]^-$ [1.295(17) Å],[21] $[(C_9H_{18}N_2)_2\text{-}(OSiMe_3)_2V(\mu\text{-}O)V(O)(OSiMe_3)_2]$ [1.285(3) and 1.245(4) Å],[22] and $[V(OC_6H_3Pr^i{}_2\text{-}2,6)_3(NNMe_2)]$ [1.311(4) Å].[18] However, while there is no doubt about the nature of the $NNMe_2$ ligand in **2b**, it is unusual in that the N−C distances appear to be unequal [1.401(15) and 1.502(15) Å] and that the N_β atom lies some 0.21 Å out of the plane formed by the surrounding NC_2 atoms. This appears to be an artifact of the structural determination, since the hydrazide ligand in **2c** is essentially planar, as is usually observed for these delocalized ligands.[18−22]

Hydrazide complexes are well-established intermediates in the high-yield stoichiometric conversion to ammonia of dinitrogen bound at Mo and W with phosphine coligands.[5,6] Such intermediates might also be involved in related reactions at analogous vanadium[13] and iron[23] sites and at a molybenum macrocyclic thioether site,[24] but yields of ammonia are low and the reaction pathways have not been studied in any detail. With this in mind, we attempted to protonate the hydrazide ligands in compounds **2b** and **2c** with halogen acid and to reduce them with $Zn/HOC_6H_3Pr^i{}_2$-2,6 (Hdipp), but neither protonation nor reduction was observed.

(16) Nanda, K. K.; Sinn, E.; Addison, A. W. *Inorg Chem*. **1996**, *35*, 1.
(17) (a) Edema, J. J. H.; Meetsma, A.; Gambarotta, S. *J. Am. Chem. Soc*. **1989**, *111*, 6878. (b) Berno, P.; Hao, S.; Minhas, R.; Gambarotta, S. *J. Am. Chem. Soc*. **1994**, *116*, 7417. (c) Buijink, J.-K. F.; Meetsma, A.; Teuben, J. H. *Organometallics* **1993**, *12*, 2004. (d) Ferguson, R.; Solari, E.; Floriani, C.; Osella, D.; Ravera, M.; Re, N.; Chiesa-Villa, A.; Rizzoli, C. *J. Am. Chem. Soc*. **1998**, *119*, 10104.
(18) Henderson, R. A.; Janas, Z.; Jerzykiewicz, L.; Richards, R. L.; Sobota, P. *Inorg, Chim. Acta* **1998**, *285*, 178.
(19) Dilworth, J. R.; Gibson, V. C.; Lu, C.; Miller, J. R.; Redshaw, C.; Zheng, Y. *J. Chem. Soc., Dalton Trans*. **1997**, 269 and references therein.
(20) Veith, M. *Angew. Chem., Int. Ed. Engl*. **1976**, *15*, 387.
(21) Bultitude, J.; Larkworthy, L. F.; Povey, D. C.; Smith, G. W.; Dilworth, J. R.; Leigh, G. J. *J. Chem. Soc., Chem. Commun*. **1986**, 1748.
(22) Danopoulos, A. A.; Hay-Motherwell, R. S.; Sweet, T. K. N.; Hursthouse, M. B. *Polyhedron* **1997**, *16*, 1081 and references therein.
(23) Hall, D. A.; Leigh, G. J. *J. Chem. Soc., Dalton Trans*. **1996**, 3539.

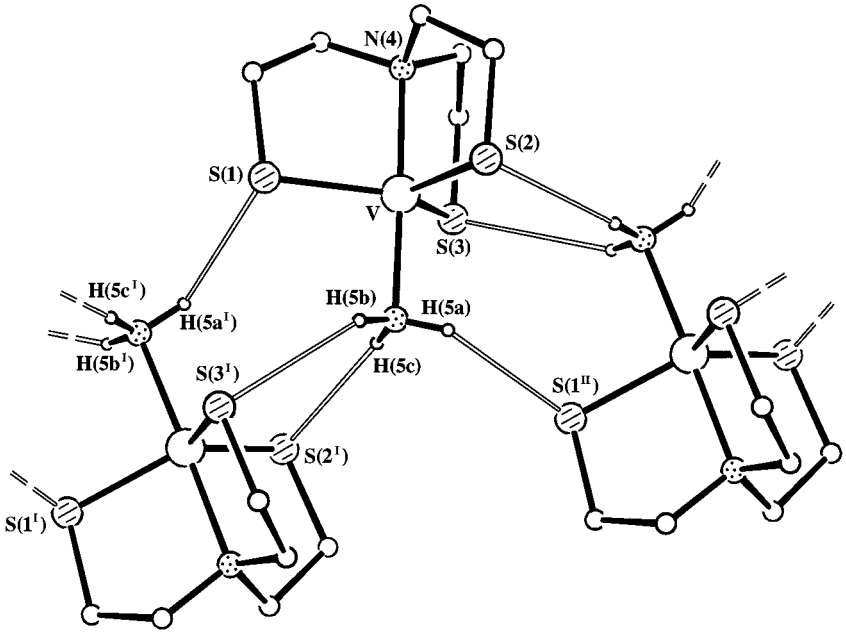

Figure 3. Proposed hydrogen bonds in crystals of [V(NS_3)(NH_3)] (**6**).

Reactions of [V(NS_3)(NH_2NH_2)] (4) and [V(NS_3)(NH_3)] (6). The reactivity of **4** has been investigated primarily with regard to the disproportionation and reduction of the hydrazine ligand, since reduction of hydrazine is catalyzed, albeit rather slowly, at VS_3 cluster sites[8] and both reduction and disproportionation of hydrazine are catalyzed at cluster[25] and mononuclear[26] MoS_3 sites.

When **4** is heated in suspension in tetrahydrofuran, a disproportionation reaction takes place and a yellow solution results from which [V(NS_3)(NH_3)] (**6**) crystallizes on cooling:

$$3[\mathrm{V}(NS_3)(\mathrm{NH_2NH_2})]\ (\mathbf{4}) \xrightarrow[\mathrm{THF}]{70\ ^\circ\mathrm{C}} 3[\mathrm{V}(NS_3)(\mathrm{NH_3})]\ (\mathbf{6}) + \mathrm{N_2} + \mathrm{NH_3} \quad (2)$$

The stoichiometry of reaction 2 has been established by quantitative measurement of all products (see Experimental Section).

However, despite this stoichiometric disproportionation reaction, complex **4** does not act as a catalyst for the disproportionation of hydrazine nor does it act as a catalyst for its reduction by Zn/Hdipp (see Experimental Section). This contrasts to some extent with the behavior of the VS_3 clusters $[Fe_3S_4X_3V(DMF)_3]^-$ (X = Cl, Br, or I), which catalyze reduction of hydrazine,[8] although not its disproportionation.

The X-ray structure of **6** shows a disordered NS_3 ligand (as in Figure 2) and an apically ligated NH_3 group. As expected, the V−NH_3 distance in **6** [2.154(7) Å] is much longer than the V−NNR^2_2 distances in **2b** [1.681(3) Å] and **2c** [1.682(2) Å], and the V−NS_3 distance, 2.155(8) Å in **6**, is correspondingly shorter than the V−NS_3 distance in **2b** [2.214(3)]Å and **2c** [2.218(2)]Å], which approach that in [VO(NS_3)] [**1**; 2.291(6) Å].[16] Individual molecules of **6** are held in chains by hydrogen bonds between the three hydrogen atoms of the ammine ligand and the S atoms of neighboring molecules as shown in Figure 3.

Compound **6** is itself thermally unstable and slowly releases NH_3 to give the poorly soluble compound formulated as [{V(NS_3)}$_n$] (**5**),

$$\mathbf{6} \xrightarrow[\mathrm{reflux}]{\mathrm{MeOH}} [\{\mathrm{V}(NS_3)\}_n]\ (\mathbf{5}) + \mathrm{NH_3} \quad (3)$$

which was also formed by a different route as shown in step 1d of Scheme 1. Presumably, **5** is at least dimeric because of bridging sulfur ligation, and it is essentially a pit into which most vanadium(III)−NS_3 species tend to fall in the absence of ligands that are able to bind the vanadium sufficiently strongly to prevent formation of sulfur bridges (see below). Direct synthesis of **5** can be achieved by treatment of **1** with $AlEt_2$(OEt),

$$\mathbf{1} \xrightarrow[\mathrm{AlEt_2(OEt)}]{\mathrm{MeCN}} [\{\mathrm{V}(NS_3)\}_n]\ (\mathbf{5}) \quad (4)$$

or by reaction of $[VCl_3(THF)_3]$ with NS_3H_3 and $LiBu^n$,

$$[\mathrm{VCl_3(THF)_3}] + NS_3\mathrm{H_3} \xrightarrow[\mathrm{LiBu^n}]{\mathrm{THF}} [\{\mathrm{V}(NS_3)\}_n]\ (\mathbf{5}) + 3\mathrm{LiCl} \quad (5)$$

Once formed, compound **5** does not react with ligands such as NH_3 and MeCN, but adducts of the V(NS_3) unit can be synthesized readily by alternative routes from compounds **4** and **6**. Thus, compound **4** reacts with anions to give the salts [NR^3_4]-[V(NS_3)X] (X = Cl, R^3 = Et, **7a**; X = Cl, R^3 = Ph, **7b**; X = Br, R^3 = Et, **7c**; X = N_3, R^3 = Bu^n, **7d**; X = N_3, R^3 = Et, **7e**; X = CN, R^3 = Et, **7f**):

$$\mathbf{4} + [\mathrm{NR^3_4}]\mathrm{X} \xrightarrow{\mathrm{MeCN}} [\mathrm{NR^3_4}][\mathrm{V}(NS_3)\mathrm{X}]\ (\mathbf{7a}-\mathbf{f}) + \mathrm{N_2H_4} \quad (6)$$

The X-ray structure of one example of this series, **7a**, was determined and shows a disordered molecule similar to that shown in Figure 2, with a chloride ligand in the apical position. The anion has the usual trigonal bipyramidal geometry with a V−N distance of 2.183(3) Å and a V−Cl distance of 2.369(1) Å. Compounds **7a**−**f** can also be obtained by displacement of NH_3 from **6** by anions. It is also to be noted that although use of **4** and a small excesss of [NEt_4]CN in reaction 6 gives **7f** in

(24) Yoshida, T.; Adachi, T.; Ueda, T.; Kaminaka, M.; Sasaki, N.; Higuchi, T.; Aoshima, T.; Mega, I.; Mizobe, Y.; Hidai, M. *Angew. Chem., Int. Ed. Engl.* **1989**, *28*, 1040.
(25) Demadis, K. D.; Coucouvanis, D. *Inorg. Chem.* **1994**, *33*, 4195.

high yield, if a ratio of **4** to $[NEt_4]CN$ of 2:1 is used in the reaction, the dinuclear compound $[\{V(NS_3)\}_2(\mu\text{-CN})]$ results,[11] which will be described elsewhere.

Displacement of NH_3 from **6** by L,

$$[V(NS_3)(NH_3)]\ (\mathbf{6}) + L \rightarrow [V(NS_3)L]\ (\mathbf{8}) + NH_3 \quad (7)$$

(L = MeCN, **8a**; L = Bu^{t}NC, **8b;** L = C_6H_{11}NC, **8c**) gives the adducts $[V(NS_3)(L)]$ [L = MeCN, ν_{CN} 2264 cm^{-1} (2254 cm^{-1} for free ligand), **8a**; L = Bu^{t}NC, ν_{NC} 2173 cm^{-1} (2136 cm^{-1} for free ligand), **8b**; L = C_6H_{11}NC, ν_{NC} 2173 cm^{-1} (2136 cm^{-1} for free ligand), **8c**], but no such displacement occurs for N_2, H_2, C_2H_2, or CO. It is worth noting at this point that a similar pattern of reactivity has been observed by Schrock and coworkers for the related vanadium sites $V(NN_3)$ [NN_3^{3-} = $\{N(CH_2CH_2NR)_3\}^{3-}$ (R = C_6F_5, $SiMe_3$, etc.)].[27] Unlike the $V(NS_3)$ site in compound **5**, the $V(NN_3)$ sites can exist as monomers for steric reasons and because nitrogen is not such a potent bridging atom as sulfur. Nevertheless, the $V(NN_3)$ sites resemble the $V(NS_3)$ site in that although they bind anions, MeCN, and Bu^{t}NC, they do not bind CO, N_2, or H_2.[27] Thus, although ligands designed to give steric constraint can limit competing interactions with the vanadium, clearly it is the electronic condition of the metal site that is of prime importance in determining whether CO, N_2, or H_2 interacts with it.

The structure of trigonal-bipyramidal compound **8a** shows an ordered molecule similar to that in Figure 1. It has an essentially linear N−V−N−C−C group, and the V−N distances of 2.147(2) Å (to the NS_3 ligand) and 2.097(2) Å (to the NCMe ligand) are the shortest of their type in Table 1.

Imide Complexes. Treatment of **4** with $SiMe_3N_3$ gives the diamagnetic imido complex $[V(NS_3)(NSiMe_3)]$ (**9**) as shown in reaction 8. The all-nitrogen-donor analogue $[V\{N(CH_2CH_2NSiMe_3)_3\}(NSiMe_3)]$ is known. [27]

$$\mathbf{4} + SiMe_3N_3 \xrightarrow[80\ ^\circ C]{MeCN} [V(NS_3)(NSiMe_3)]\ (\mathbf{9}) + N_2 + N_2H_4 \quad (8)$$

Complex **9** is a useful precursor to a range of other imide complexes. Thus, it can be smoothly hydrolyzed to the imide complex **10** (reaction 9) and reacts with $ClCPh_3$ to give $[V(NS_3)(NCPh_3)]$ (**11**) [reaction 10]. Complex **10** reacts with $[NMe_4]OH$ to regenerate $[V(NS_3)O]$ (**1**) [reaction 11] and with LiN(i-Pr) to give $[V(NS_3)\{NLi(THF)_2\}]$ (**12**) [reaction 12].

$$\mathbf{9} \xrightarrow[20\ ^\circ C]{MeCN/H_2O} [V(NS_3)(NH)]\ (\mathbf{10}) \quad (9)$$

$$\mathbf{9} + ClCPh_3 \xrightarrow[reflux]{MeCN} [V(NS_3)(NCPh_3)]\ (\mathbf{11}) + SiMe_3Cl \quad (10)$$

$$\mathbf{10} \xrightarrow[60\ ^\circ C]{[NMe_4]OH/MeOH} [V(NS_3)O]\ (\mathbf{1}) \quad (11)$$

$$\mathbf{10} \xrightarrow[THF/20\ ^\circ C]{LiNPr^i} [V(NS_3)\{NLi(THF)_2\}]\ (\mathbf{12}) \quad (12)$$

A further range of imido complexes $[V(NS_3)(NR^4)]$ (R^4 = C_6H_4Y-4, where Y = H (**13a**), OMe (**13b**), Me (**13c**), Cl (**13d**), Br (**13e**), NO_2 (**13f**); R^4 = C_6H_4Y-3, where Y = OMe (**13g**), Cl (**13h**); R^4 = $C_6H_3Y_2$-3,4, where Y = Me (**13i**), Cl (**13j**), R^4 = C_6H_{11} (**13k**)) have also been prepared by the well-known route[28]

$$[V(NS_3)O]\ (\mathbf{1}) + R^4NCO \rightarrow [V(NS_3)(NR^4)]\ (\mathbf{13a-k}) + CO_2 \quad (13)$$

The conditions of reaction 13 generally involve high temperature, with the isocyanate itself or 2-methoxyethanol as solvent, which demonstrates the robust nature of these imide complexes.

The X-ray structures of compounds **9**, **10**, and **13d** have been determined and take the same form as complex **4** (Figure 1). They all have the expected trigonal bipyramidal geometry with variations in the fifth apical ligand site. The V−imide distance of **9**, mean value of 1.645(3) Å, is somewhat shorter than that of $[V(C_5H_5)_2(NSiMe_3)]$[29] (1.665 Å) but longer than in $[VCl_3(NSiMe_3)]$[30] (1.59 Å) and in the usual range for imide complexes generally (1.59−1.73 Å), which are regarded as having close to a triple bond between the metal and the imide nitrogen.[27−31] The corresponding distances in **10** and **13d** are 1.638(3) Å and 1.670(2) Å, respectively. Compound **10** is a further example of the relatively rare class of NH complexes; an analogue $[V\{N(CH_2CH_2NSiMe_3)_3\}(NH)]$[27] is known that has a V−N distance [1.638(6) Å] identical to that of **10**. In both $[V\{N(CH_2CH_2NSiMe_3)_3\}(NH)]$ and **10**, the imido hydrogen has been located and refined, showing, in both cases, that the V−N−H angle is close to linear [173(6)° and 179(3)°, respectively] and that the N−H distances are essentially identical [0.79(7) and 0.80(4) Å, respectively]. A difference between the structures is due to sulfur ligation, in that **10** shows a hydrogen bonding interaction in the solid state between the hydrogen atom of the NH group and an S atom in a neighboring molecule, thus linking molecules in pairs about a center of symmetry (Figure 4).

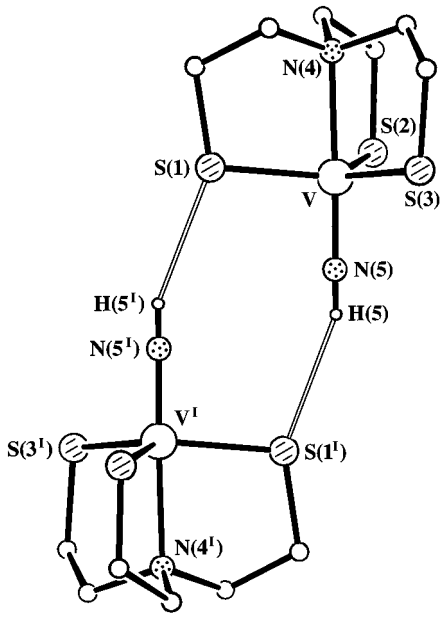

Figure 4. Hydrogen-bonded dimer units of $[V(NS_3)(NH)]$ (**10**).

General Structural Considerations of NS_3 Complexes. The range of structurally related compounds that we have obtained,

(26) Hitchcock, P. B.; Hughes, D. L.; Maguire, M. J.; Marjani, K.; Richards, R. L. *J. Chem. Soc., Dalton Trans*. **1997**, 4747.
(27) Cummins, C. C.; Schrock, R. R.; Davis, W. M. *Inorg. Chem*. **1994**, *33*, 1448.
(28) Devore, D. D.; Lichtenhan, J. D.; Takusagawa, F.; Maatta, E. A. *J. Am. Chem. Soc*. **1987**, *109*, 6878 and references therein.
(29) Wiberg, N.; Haring, H. W.; Schubert, U. *Z. Naturforsch*. **1980**, *356*, 599.
(30) Schweda, E.; Scherfise, K. D.; Dehnicke, K. *Z. Anorg. Allg. Chem.* **1985**, *528*, 117.
(31) Nugent, W. A.; Mayer, J. M. *Metal−Ligand Multiple Bonds*; Wiley-Interscience: New York, 1988.

$[V(NS_3)Z]$, allows comparison of bond parameters within two series of complexes that have a formally different oxidation state at vanadium, paramagnetic $[V^{III}(NS_3)Z^1]$ ($Z^1 = NH_2NH_2$, NH_3, MeCN, and Cl^-) and diamagnetic $[V^V(NS_3)Z^2]$ (Z^2 = O, $NNMe_2$, NNMePh, $NSiMe_3$, NH, and NC_6H_4Cl-4). For the series $[V^{III}(NS_3)Z^1]$, the V−N distances trans to the group Z^1 (d(V−NS_3)) span the range 2.147−2.183 Å (Table 1) and give an order of trans influence (trans bond lengthening) for Z^1 of $Cl^- > NH_3 \sim N_2H_4 > CH_3CN$. Similarly, for the series $[V^V(NS_3)Z^2]$ the distances (d(V−NS_3)) span the range 2.214−2.291 Å and give an order of trans influence for Z^2 of O > $NSiMe_3$ > NH > NC_6H_4Cl-4 > $NNMe_2 \sim$ NNMePh. Within the series $[V(NS_3)NR^4]$ ($R^4 = SiMe_3$, H, or C_6H_4Cl-4), as the V═NR^4 distances decrease in the order C_6H_4Cl-4 > $SiMe_3$ > H, the corresponding distances (d(V−NS_3)) increase in the order C_6H_4Cl-4 < H < $SiMe_3$ (Table 1). Although the detailed order is not precisely matched, this trend is as expected for the coupled N−V═NR^4 system.

For $[V^V(NS_3)Z^2]$, as the V−NS_3 distances increase, the average V−S distances correspondingly decrease, as might be expected for this tripodal ligand (Table 1). This rule does not appear to be followed for $[V^{III}(NS_3)Z^1]$, but in this series the distances for $Z^1 = NH_3$, N_2H_4, and CH_3CN are all similar and the anionic charge of the complex when $Z^1 = Cl^-$ presumably lengthens all bonds to the NS_3 ligand.

Considering both series, we note that the d(V−NS_3) values for the series $[V^V(NS_3)Z^2]$ are greater than those for $[V^{III}(NS_3)Z^1]$, despite the smaller ionic radius for V^V (ionic radius of V^V = 0.68 Å, ionic radius of V^{III} = 0.78 Å); i.e., the Z^2 ligands have the greater trans bond weakening ability. The highest in trans influence is the oxide ligand followed by imide ligands, which is not unexpected in view of their good σ-donor power and π-releasing ability.[31] Hydrazides, being good σ-donors and π-releasing ligands,[32] also have a relatively strong trans influence. Lowest in the series is CH_3CN, entirely in keeping with its overall weakness as a ligand.[33]

Complexes of the $[O(CH_2CH_2S)_2]^{2-}$/$[OS_2]^{2-}$ Ligand. Because the ligation of vanadium in nitrogenase appears to involve oxygen (from homocitrate) as well as sulfur and nitrogen, we were interested in forming a robust system that would have oxygen as well as sulfur ligation, and for our initial investigation we have explored some vanadium chemistry of the $[OS_2]^{2-}$ ligand. Apart from the variation of ligand donor atoms that this system gives us compared to $[NS_3]^{3-}$, the $[OS_2]^{2-}$ ligand confers a lower coordination number on vanadium so that not only the nitrogen-donor ligands of choice (hydrazide, imide, etc.) can be attached to the vanadium but also a variety of other coligands, such as phenoxide in the examples given in this paper.

Preparations and Structures. As a precursor to the desired hydrazide and imide complexes, we prepared the oxide complex $[V(OS_2)O(dipp)]$ (**14**; dipp = $OC_6H_3Pr^i_2$-2,6) from $[VO(OPr^i)_3]$, Hdipp, and OS_2H_2 as shown in reaction 14.

$$[VO(OPr^i)_3] + \text{Hdipp} + OS_2H_2 \xrightarrow[20\ ^\circ C]{\text{hexane}} [V(OS_2)O(dipp)]\ (\mathbf{14}) + 3HOPr^i \quad (14)$$

Red, diamagnetic **14** has ν(VO) at 982 cm^{-1}, and its X-ray structure is shown in Figure 5. It has essentially trigonal bipyramidal geometry with the trigonal plane formed by the oxygen atom of the dipp ligand and the two sulfur atoms of the $[OS_2]^{2-}$ group. The V═O distance [1.573(2) Å] is very close to that of **1** [1.578(6) Å] and is in the range expected for this type of compound. Other features of the structure are unexceptional. Compound **14** reacts with NH_2NMe_2 to give $[V(OS_2)(NNMe_2)(dipp)]$ (**15**),

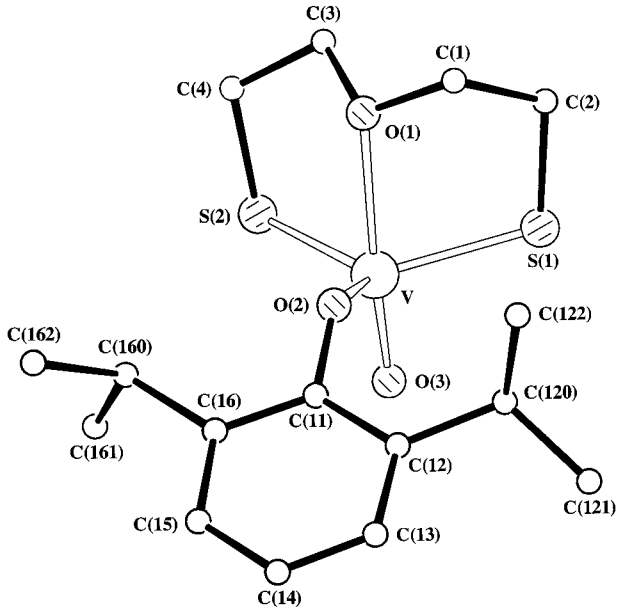

Figure 5. Molecule of $[V(OS_2)O(dipp)]$ (**14**).

$$\mathbf{14} + NH_2NMe_2 \xrightarrow{CH_3CN} [V(OS_2)(NNMe_2)(dipp)]\ (\mathbf{15}) + H_2O \quad (15)$$

and with $(SiMe_3)_2NH$ to give $[V(OS_2)(NSiMe_3)(dipp)]$ (**16**),

$$\mathbf{14} + (SiMe_3)_2NH \xrightarrow{CH_3CN} [V(OS_2)(NSiMe_3)(dipp)]\ (\mathbf{16}) + HOSiMe_3 \quad (16)$$

A second oxide precursor, formulated as $[V(OS_2)_{1.5}O]$ (**17**), has also been obtained,

$$[VO(OPr^i)_3] + 1.5OS_2H_2 \xrightarrow[20\ ^\circ C]{\text{hexane}} [V(OS_2)_{1.5}O]\ (\mathbf{17}) + 3HOPr^i \quad (17)$$

and it reacts with $SiMe_3NHNMe_2$ to give $[V(OS_2)(NNMe_2)(OSiMe_3)]$ (**18**),

$$\mathbf{17} + NH(SiMe_3)NMe_2 \xrightarrow{CH_3CN} [V(OS_2)(NNMe_2)(OSiMe_3)]\ (\mathbf{18}) + 0.5H_2OS_2 \quad (18)$$

The X-ray structures of **15**, **16**, and **18** are very similar to that of **14** (Figure 5). All the $V(OS_2)$ compounds have the expected trigonal bipyramidal structure with two sulfur atoms of the $[OS_2]^{2-}$ ligand and one oxygen atom of the dipp (**14**, **15**, and **16)** or $OSiMe_3$ (**18**) ligand defining the trigonal plane. The axial system in **14**−**16** consists of the O−V−Z^3 group in the series $[V^V(OS_2)Z^3(dipp)]$, where O is the central oxygen of the $[OS_2]^{2-}$ ligand and Z^3 = O, $NNMe_2$, or $NSiMe_3$. Therefore, we have again a trans influence system, as in the $[V^V(NS_3)Z^2]$ series above, which gives for V−O(OS_2) lengthening the same trans influence order, O > $NSiMe_3$ > $NNMe_2$, as was seen for V−N lengthening in $[V^V(NS_3)Z^2]$ (Table 1). Also, in parallel with trends in the NS_3 series, the V−S distances in $[V^V(OS_2)$-

(32) Chatt, J.; Fakley, M. E.; Hitchcock, P. B.; Richards, R. L.; Luong-Thi, N. T. *J. Chem. Soc., Dalton Trans.* **1982**, 345.
(33) Ihmels, K.; Rehder, D. *Organometallics* **1985**, *4*, 1340.

Table 4. ^{51}V NMR and Electronic Spectra of [V(^{t}*NS*$_3$)Z^2] and [V(*OS*$_2$)Z^3(dipp)] in CH_2Cl_2

no.	Z^2 or Z^3	^{51}V (ppm)	λ_1 (nm)	λ_2 (nm)
		[V(^{t}*NS*$_3$)Z^2]		
1	O	557	356	503
2c	NNMePh	446		
2d	NNHPh	420		
2b	$NNMe_2$	416		
13f	$NC_6H_4NO_2$-4	355		
9	$NSiMe_3$	349	380	448
13j	$NC_6H_3Cl_2$-3,4	337	332	453
13b	NC_6H_4OMe-4	335	329	444
13d	NC_6H_4Cl-4	331	328	449
13e	NC_6H_4Br-4	331	330	448
13h	NC_6H_4Cl-3	328	329	452
13c	NC_6H_4Me-4	325	327	445
13i	$NC_6H_3Me_2$-3,4	325	325	444
13g	NC_6H_4OMe-3	322	332	450
13a	NPh	321	323	448
11	$NCPh_3$	234	329	446
10	NH	210	331	454
13k	NC_6H_{11}	194		
		[V(*OS*$_2$)Z^3(dipp)]		
15	$NNMe_2$	269		
14	O	191		
16	$NSiMe_3$	61		

Z^3(dipp)] increase as the axial V−O(*OS*$_2$) distance decreases. The equatorial V−O distances in **14**−**16** and **18**, which span the range 1.785−1.808 Å, are shorter than the corresponding axial V−O distances, no doubt a consequence of the proximity of neighboring ligands in the five coordinate complexes and the anionic nature and stronger binding of the equatorial phenoxide or alkoxide oxygen compared to the ether-type oxygen of the axial linkage. The spectroscopic and other physical properties of complexes **14**−**18** are given in the Experimental Section.

^{51}V NMR and Electronic Spectra of Complexes. ^{51}V NMR spectroscopy is a convenient and powerful tool with which to examine vanadium complexes and, in conjunction with UV/visible spectroscopy, to probe the electronic manifold of such compounds. In particular, Rehder has mapped the ^{51}V chemical shifts corresponding to the vanadium environment[33,34] and Maata has used ^{51}V NMR spectroscopy and UV/visible spectroscopy to study vanadium oxide and imide compounds.[28] In these studies, the vanadium chemical shift was shown in general to move to low field (relative to a chosen standard, $VOCl_3$) as the electronegativity of nonpolarizable ligands at vanadium decreased, thus decreasing the mean HOMO−LUMO gap, ΔE, and increasing the paramagnetic shielding term σ. Ligands that participate in low-energy ligand-to-metal charge transfer cause a reduction of ΔE and hence additional deshielding.[28,33,34] As might be expected on this basis, because of the presence of the highly polarizable sulfur ligands, all the compounds [V(*NS*$_3$)Z^2] (Z^2 = O, NR, or NNR_2) of this study show shifts downfield of $VOCl_3$ and the resonances of the *NS*$_3$ complex series (VNS_3L ligation) are to the low field of the corresponding members of the *OS*$_2$ series (VO_2S_2L ligation) (Table 4). Illustrative of this general trend are the ^{51}V shifts (ppm) of the analogous pairs of compounds: [V(*NS*$_3$)O] 564; [V(*OS*$_2$)O($OC_6H_3Pr^i_2$-2,6)] 191; [V(*NS*$_3$)($NNMe_2$)] 418; [V(*OS*$_2$)($OC_6H_3Pr^i_2$-2,6)$_3$($NNMe_2$)] 269.

Within the [V(*NS*$_3$)Z^2] series, the order of the Z^2 ligands in terms of ^{51}V chemical shift (greatest deshielding) is O (557) > NNR_2 (416−446) > NR (194−355). For the series [V(*OS*$_3$)($OC_6H_3Pr^i_2$-2,6)Z^2], the corresponding order is NNR_2 (269) > O (191) > NR(61). Here, we note that the order for both series does not follow that expected simply from electronegativities,[28,33,34] where the position for Z^2 = O would be expected to be to the high field of the nitrogen ligands, as is seen for the series [V{N($CH_2CH_2NSiMe_3$)$_3$}Z] (Z = O or NR).[27]

Within the imide series [V(*NS*$_3$)(NR^5)] (R^5 = H, $SiMe_3$, C_6H_{11}, CPh_3, or R^4) the order (ppm) of deshielding with imide substituent is R^4 (321−355) ≥ $SiMe_3$ (349) > CPh_3 (234) > H (210) > C_6H_{11} (194). Thus, there is a greater deshielding for imides carrying aryl as opposed to alkyl groups. The same trend was also observed for the four coordinate series [VCl_3(NR^6)] (R^6 = alkyl or aryl) and was attributed to a reduction of ΔE and hence greater deshielding for complexes having aryl substituents because the HOMO for these compounds is destabilized as a result of a considerable N−C(aryl) π* component.[28]

There is a relatively very small spread of resonances (321−355 ppm) within the series [V(*NS*$_3$)(NR^4)] (R^4 = C_6H_4Y-4, where Y = H, OMe, Me, Cl, Br, or NO_2). Evidently, variation of the electronic nature of the aryl substituent has only a minor effect on the shielding at vanadium (Table 4). Plots of ^{51}V shift versus Hammett σ constants, Taft σ_I constants, and Swain's *F* values for the substituents Y show little correlation (data not shown). This contrasts with the larger effect of substituent on the ^{51}V resonances of the series [VCl_3(NR^6)], which span the range 182−403 ppm.[28] Presumably the higher coordination number of the [V(*NS*$_3$)(NR^4)] series and the buffering effect of their sulfur ligands contribute to the relatively small range of resonance for these compounds.

All the V^V(*NS*$_3$) compounds we have studied show two prominent absorptions in the UV/vis region [λ_1 (at lower frequency) and λ_2; Table 4], as do members of the series [VCl_3(NR^4)].[28] Since these absorptions are related to ΔE, they should also correlate with the ^{51}V shifts. A correlation with λ_1 has been observed for the [VCl_3(NR^4)] series; as Cl is replaced by the more electronegative OAr or OBu^t, λ_1 shifts to higher energy and the ^{51}V shift moves to higher field.[28] In the case of our [V^V(*NS*$_3$)Z^2] complexes, as Z^2 is changed from O to NR, the ^{51}V shift moves to higher field and λ_1 and λ_2 in general move to higher energy (Table 4). There is little variation in λ_1 and λ_2 across the imide series.

In conclusion, although the variation of ^{51}V shift with electronic transitions and thus ΔE appear to be internally consistent within our [V(*NS*$_3$)Z^2] series, the relative position of the oxides [V(*NS*$_3$)O] and [V(*OS*$_2$)($OC_6H_3Pr^i_2$-2,6)O] are unexpectedly low field with respect to complexes of nitrogen donors, which have lower electronegativity than oxide. In the absence of detailed theoretical studies, it is not clear what factors influence ΔE to give rise to this apparent anomaly, but clearly, it is a consequence of the presence of the *NS*$_3$ ligand, since the analogues [V{N($CH_2CH_2NSiMe_3$)$_3$}Z][27] follow the expected order of electronegativities.

Conclusion

The reaction of the V=O unit in **1** and **14**, particularly with hydrazines but also other reagents, has allowed access to a range of vanadium complexes with various NR (NR = N_2H_4, NH_3, NH, etc.) ligands at V*NS*$_3$ and V*OS*$_2$ sites. However, although these vanadium sites are adept at binding nitrogenous species that could be involved in the latter stages of fixation of N_2 at the vanadium site of vanadium nitrogenase, they are incapable of binding N_2 or other substrates or inhibitors of nitrogenase such as CO or H_2. Similar behavior is seen for their *NN*$_3^{3-}$ analogues.[27] This might be due to the inability of the V*NS*$_3$ and V*NN*$_3$ sites to match the π-acceptor requirement of a terminal

(34) Rehder, D.; Ihmels, K. *Inorg. Chim. Acta* **1983**, *76*, L313.

N_2 group. An indication of this is that although the d^2 VNS_3 site is able to bind MeCN in **8a** and RNC in **8b** and **8c**, in these compounds the NC and CN stretching frequencies are slightly increased compared to those in the free ligands, whereas these frequencies generally decrease when these ligands coordinate sites capable of binding CO or N_2.[35] For example, the d^4 compound [Re(*NS*$_3$)(CNBu^t)] shows a decrease of ν(NC) of 161 cm^{-1} relative to that of free CNBu^t, and [Re(*NS*$_3$)(CO)] can be prepared.[36]

The geometry of the VNS_3 site would also accommodate the bridging mode of N_2 binding, and we have presented some evidence that this does occur weakly, but it might be necessary to lower the oxidation state of the vanadium to make VNS_3, or a related site, sufficiently electron-releasing to accomplish stable N_2 binding in either the terminal or the bridging mode. We have observed that ligands other than N_2 bind strongly in the bridging mode. For example, we have obtained the dinuclear compounds NBu$_4$[(*NS*$_3$)V(μ-CN)V(*NS*$_3$)] and NEt$_4$[(*NS*$_3$)V(μ-N)V(*NS*$_3$)].[11] The properties of these and related complexes will be discussed in detail elsewhere.

Experimental Section

General Information. All operations were carried out under a dry dinitrogen atmosphere, using standard Schlenk techniques. All the solvents were distilled under dinitrogen from the appropriate drying agents prior to use. The compound $Me_3SiNHNMe_2$ was prepared by a literature method.[37] All other starting materials were obtained from the Aldrich Chemical Co. and used without further purification unless stated otherwise. Infrared spectra were recorded on a Perkin-Elmer 180, Perkin-Elmer 883, or Shimadzu FTIR-8101M instrument in Nujol mulls and UV/vis spectra on a Shimadzu UV-2101 PC spectrophotometer. ^{1}H, ^{13}C, ^{14}N, and ^{51}V NMR spectra were measured on a JEOL GSX 270, JEOL JNM-LA400, or Bruker ESP 300E spectrometer (^{1}H and ^{13}C ref $SiMe_4$, ^{14}N ref CH_3NO_2, ^{51}V ref $VOCl_3$). Standard heteronuclear multiquantum coherence, heteronuclear multibond correlation, and other 2-D techniques were used as appropriate in the assignment of spectra. Magnetic moment determinations were either in the solid state, using a Johnson−Matthey Gouy balance, or in solution by ^{1}H NMR using the Evans method.[38] Microanalyses were by Mr. A Saunders of the University of East Anglia, U.K. or at the University of Wroclaw, Poland.

Preparation of N(CH$_2$CH$_2$SH)$_3$[*NS*$_3$H$_3$]. A modification of the literature method was used. Batches of tris(chloroethyl)amine hydrochloride[39] (*CAUTION: VESICANT*) were made from 60 g batches of triethanolamine and converted the same day to tris[2-(*S*-isothiaureido)-ethyl]amine tetrahydrochloride.[40] *This work was carried out in enclosed Schlenk apparatus while wearing heavy duty gloves and a face mask.* The tetrahydrochloride was treated in 0.05 or 0.1 mol batches with sodium hydroxide,[41] giving tris(mercaptoethyl)amine NS_3H_3. The crude product was not purified by distillation or by conversion to its hydrochloride, but rather it was dissolved in diethyl ether and filtered to remove a white solid, and the ether was removed from the filtrate in vacuo. The overall yield of NS_3H_3 from triethanolamine was 30−40%.

Preparation of [V(*NS*$_3$)O] (1). Following Nanda et al.,[16] NS_3H_3 (9 g, ∼45 mmol) was added to diethyl ether (45 cm^3) at 20 °C and the mixture stirred quickly. [VO(OPr^i)$_3$] (10 g, 41 mmol) was added dropwise giving a red precipitate that was filtered off in air, washed with ether, and Soxhlet extracted under dinitrogen with hot acetonitrile (∼150 cm^3) until a small green residue remained (∼4 h). Ether (150 cm^3) was added to the cooled extract, and it was kept at −20 °C for 1 h. The resulting purple crystals were filtered off in air, washed with acetonitrile−ether and then ether, and dried in vacuo (yield 8.2 g, 31 mmol, 77%). Anal. Calcd for $C_6H_{12}NOS_3V$: C, 27.6; H, 4.6; N, 5.4. Found: C, 27.7; H, 4.5; N, 5.3.

Preparation of [V(*NS*$_3$)(NNMe$_2$)] (2b). (a) Method A. [V(dipp)$_3$(NNMe$_2$)][18] (0.3 g, 0.46 mmol) was dissolved in hexane, and NS_3H_3 (0.08 cm^3, 0.46 mmol) was added. The mixture was stirred overnight at ambient temperature to give a red solid that was filtered off and recrystallized from MeCN to give bright-red crystals that were suitable for crystallographic study. Anal. Calcd for $C_8H_{18}N_3S_3V$: C, 31.7; H, 5.9; N, 13.9. Found: C, 31.4; H, 5.8; N, 13.6. ^{1}H NMR (CD_3CN): ∂ 3.33 (t, 6H, NCH_2CH_2S, $^3J_{H-H}$ 5.5 Hz), 3.43 (s, 6H NCH_3), 3.51 (m, 6H, NCH_2CH_2S). ^{13}C NMR (CD_3CN): ∂ 34.61 (NCH_2CH_2S), 45.16 (NCH_3), 57.91 (NCH_2CH_2S). ^{51}V NMR (CD_3CN): ∂ 416 (fwhm = 435 Hz).

(b) Method B. **1** (0.26 g, 1 mmol) and *N*,*N*-dimethylhydrazine (5 cm^3) were taken to reflux for 3 h and filtered hot. Dark-red crystals (0.16 g, 53%) of the product crystallized on cooling; they were filtered off, washed with diethyl ether, and dried in vacuo. They were shown to be identical to those obtained by method A by spectroscopy and analysis.

(c) Method C. **1** (0.26 g, 1 mmol) and ($SiMe_3$)NHNMe$_2$ (10 mmol) were heated under reflux in CH_3CN (25 cm^3) for 48 h. Cooling to 4 °C gave red crystals (0.2 g, 66%), shown to be identical to those obtained by method A by spectroscopy and analysis.

Preparation of [V(*NS*$_3$)(NNMePh)] (2c). The preparation of **2c** was as for **2b** (method C), but using ($SiMe_3$)NHNMePh, and gave red crystals suitable for X-ray analysis (65%). Anal. Calcd for $C_{13}H_{20}N_3S_3V$: C, 42.8; H,5.5; N, 11.5. Found: C, 41.8; H, 5.7; N, 11.8. ^{1}H NMR (CD_3CN): ∂ 3.36 (t, 6H, NCH_2CH_2S, $^3J_{H-H}$ 5.5 Hz), 3.63 (m, 6H, NCH_2CH_2S), 4.06 (s, 6H, NCH_3), 7.03−7.61 (m, 5H, Ph). ^{13}C NMR (CD_2Cl_2): ∂ 33.95 (NCH_2CH_2S), 39.2 (NCH_3), 57.11 (NCH_2CH_2S), 113.3, 123.0, 129.1 (NC$_6$H$_5$). ^{51}V NMR (CD_3CN): ∂ 446 (fwhm = 606 Hz).

Preparation of [V(*NS*$_3$)(NNHPh)] (2d). Phenylhydrazine (8 cm^3, excess) was added to **1** (1.31 g, 5 mmol). The mixture was heated in vacuo to 150 °C for 10 min, whereupon the purple color became orange-red. It was cooled and filtered, leaving a very small residue; diethyl ether (40 cm^3) was added as a layer to the filtrate. Dark-red crystals, suitable for X-ray studies, grew overnight and were filtered off, washed with diethyl ether, and dried in vacuo (1.55 g, 4.4 mmol, 88%). Anal. Calcd for $C_{12}H_{18}N_3S_3V$: C, 41.0; H, 5.1; N, 12.0. Found: C, 41.5; H, 5.3; N, 12.2. ^{1}H NMR (CD_3CN): ∂ 3.35 (t, 6H, NCH_2CH_2S, $^3J_{H-H}$ 5.4 Hz), 3.61 (m, 6H, NCH_2CH_2S). ^{13}C NMR (CD_3CN): ∂ 34.71 (NCH_2CH_2S), 57.96 (NCH_2CH_2S) 112.3, 124.0, 131.1 (NC$_6$H$_5$). ^{51}V NMR (CD_2Cl_2): ∂ 420 (fwhm = 730 Hz). IR (Nujol mull): 3066 cm^{-1} (m, ν_{NH}).

Preparation of [V(*NS*$_3$)(NH$_2$NH$_2$)] (4). (a) Method A. Anhydrous hydrazine (6.4 g, 200 mmol) was dissolved in acetonitrile (∼100 cm^3). The solution was decanted from a small residue, then added to a suspension of **1** (12.3 g, 47 mmol) in acetonitrile (∼100 cm^3). The mixture was stirred at about 50 °C. The color of the suspension changed from red to green to yellow over about 1 h, then the mixture was cooled at −20 °C, and the resulting solid was filtered off, washed with acetonitrile and ether, and dried in vacuo (yield 12.7 g, 46 mmol, 98%).

(b) Method B. Anhydrous hydrazine (0.32 g, 10 mmol) in MeCN (100 cm^3) was added to Et$_4$N[V(*NS*$_3$)Cl] (**8a**; 0.21 g, 0.5 mmol) in MeCN (100 cm^3). The solution turned yellow, and crystals suitable for X-ray studies grew for over a week. Anal. Calcd for $C_6H_{16}N_3S_3V$: C, 26.0; H, 5.8; N,15.2. Found: C, 25.6; H, 5.7; N, 15.7. $\mu_{eff} = 2.82\mu_B$. IR (Nujol mull): 3337, 3248, 3183, 3099 cm^{-1} (m, ν_{NH}).

Preparation of {V(*NS*$_3$)}$_n$ (5). (a) Method A. **6** (0.41 g,1 mmol) was refluxed for 10 min in methanol, giving a dark-green precipitate that was filtered off from the cooled solution, washed with ether, and dried in vacuo (0.20 g, 0.82 mmol, 82%). Anal. Calcd for $C_6H_{12}NS_3V$: C, 29.4; H, 4.9; N, 5.7. Found: C, 29.4; H, 4.8; N, 6.2.

(b) Method B. **1** (0.21 g, 0.8 mmol) and diethylaluminum ethoxide (1 mL of 1.6 M toluene solution) were refluxed in acetonitrile (25 cm^3) for 30 min, then filtered hot. The resulting dark-green precipitate (0.06 g) was washed with hot acetonitrile and ether and dried in vacuo. It had an IR spectrum identical to that of **5** as prepared above.

(35) Chatt, J.; Dilworth, J. R.; Richards, R. L. *Chem. Rev.* **1978**, *78*, 589.
(36) Glaser, M.; Spies, H.; Lüger, T.; Hahn, F. E. *J. Organomet. Chem.* **1995**, *503*, C32.
(37) Chatt, J.; Crichton, B. A. L.; Dilworth, J. R.; Dahlstrom, P.; Gutkoska, R.; Zubieta, J. *Inorg. Chem.* **1982**, *21*, 2383.
(38) Evans, D. F. *J. Chem. Soc.* **1958**, 2003.
(39) Ward, K. *J. Am. Chem. Soc.* **1935**, *57*, 914.
(40) Harley-Mason, J. *J. Chem. Soc.* **1947**, 320.
(41) Barbaro, P.; Bianchini, C.; Scapacci, G.; Masi, D.; Zanello, P. *Inorg. Chem.* **1994**, *33*, 3180.

(c) Method C. NS_3H_3 (0.3 cm^3, 1.52 mmol) and Bu^{n}Li (3 cm^3, 4.5 mmol) were added simultaneously via a syringe to a solution of $[VCl_3(THF)_3]$ (0.5 g, 1.34 mmol) in THF (80 cm^3). There was an immediate reaction to give a deep-brown solution, which was taken to dryness in a vacuum to leave a green-brown solid that was washed with ether, dried, and had an IR spectrum identical to that of **5** as prepared above (0.20 g, 0.82 mmol, 63%). Anal. Calcd for $C_6H_{12}NS_3V$: C, 29.4; H, 4.9; N, 5.7. Found: C, 28.3; H, 4.8; N, 6.2.

Preparation of [V(*NS*$_3$)(NH$_3$)] (6). 4 (0.30 g, 1.1 mmol) was heated to reflux in acetonitrile (10 cm^3) and filtered from a small green residue. Yellow crystals (0.14 g, 0.53 mmol, 48% yield), suitable for X-ray studies, crystallized on cooling overnight. They were washed with acetonitrile and ether and dried in vacuo. Anal. Calcd for $C_6H_{15}N_2S_3V$: C, 27.5; H, 5.7; N, 10.7. Found: C, 27.8; H, 5.8; N, 11.1. $\mu_{eff} = 2.70\mu_B$. IR (Nujol mull): 3255, 3216, 3190, 3142 cm^{-1} (m, ν_{NH}).

Preparation of Et$_4$N[V(*NS*$_3$)Cl] (7a). Tetraethylammonium chloride hydrate (4.5 g, ~25 mmol) was dried in vacuo at 100 °C for 2 h, then mixed with **4** (5.55 g, 20 mmol). Acetonitrile (300 cm^3) was added and the mixture refluxed for 20 min, giving a red solution that was filtered hot from a small yellow residue and cooled to room-temperature overnight, then at −20 °C for 2 nights. Pink crystals suitable for X-ray studies were filtered off, washed with acetonitrile and ether, and dried in vacuo (6.95 g, 16.9 mmol, 84%). Anal. Calcd for $C_{14}H_{32}ClN_2S_3V$: C, 40.9; H,7.8; N, 6.8. Found: C, 40.9; H,7.7; N, 6.9. $\mu_{eff} = 2.91\mu_B$.

Preparation of Ph$_4$P[V(*NS*$_3$)Cl] (7b). [Ph$_4$P]Cl (0.6 g,1.6 mmol) was added to the solution formed by heating **4** (0.55 g 2 mmol) in MeCN (40 cm^3) to reflux and filtering. The [Ph$_4$P]Cl dissolved, and a brown precipitate was formed. After 2 h this was filtered off, washed with ether, and dried in vacuo (0.96 g,1.55 mol, 78%). Anal. Calcd for $C_{30}H_{32}ClN_2PS_3V$: C, 58.1; H, 5.2; N, 2.3. Found: C, 58.1; H, 6.0; N, 2.2.

Preparation of Et$_4$N[V(*NS*$_3$)Br] (7c). The preparation of **7c** was similar using [Et$_4$N]Br (0.21 g, 1 mmol) and **4** (0.27 g, 1 mmol) in MeCN (10 cm^3). Brown crystals (0.18 g, 0.4 mmol, 40%) were obtained on cooling the solution and a further 0.13 g (0.3 mmol, 30%) on adding ether (30 cm^3). Anal. Calcd for $C_{14}H_{32}BrN_2S_3V$: C, 36.9; H, 7.1; N, 6.2. Found: C, 36.5; H, 6.7; N, 6.7. $\mu_{eff} = 2.74\mu_B$.

Preparation of Bu^n$_4$N[V(*NS*$_3$)Br] (7d). Preparation of **7d** was similar using [Bu^n$_4$N]Br (0.62 g) and **4** (0.66 g, 2.4 mmol). The filtrate was reduced to dryness in vacuo, the residue was dissolved in MeCN (5 cm^3), and then ether (20 cm^3) was added, giving an oil (0.09 g, 0.16 mmol, 7%) that crystallized at −20 °C. Anal. Calcd for $C_{22}H_{48}BrN_2S_3V$: C, 46.6; H, 8.5; N, 4.9. Found: C, 46.1; H, 8.5; N, 4.9.

Preparation of Et$_4$N[V(*NS*$_3$)(N$_3$)] (7e). Preparation of **7e** was similar from [Et$_4$N]N$_3$ (0.75 g, 4.4 mmol) and **4** (1.12 g, 4 mmol) in MeCN (20 cm^3), giving 1.10 g (2.6 mmol, 66%) of red crystals. Anal. Calcd for $C_{14}H_{32}N_5S_3V$: C, 40.3; H, 7.7; N, 16.8. Found: C, 40.5; H, 7.8; N, 17.1. $\mu_{eff} = 2.53\mu_B$. IR (Nujol): 2056 cm^{-1} (s, ν_{N3}).

Preparation of Et$_4$N[V(*NS*$_3$)(CN)] (7f). Preparation of **7f** was similar from [Et$_4$N]CN (1.25 g, 8 mmol) and **4** (2.08 g, 7.5 mmol) in MeCN (150 cm^3), giving 1.66 g (4.15 mmol, 55%) of yellow crystals. Anal. Calcd for $C_{15}H_{32}N_3S_3V$: C, 44.9; H, 8.0; N, 10.5. Found: C, 45.1; H, 8.1; N, 10.5. $\mu_{eff} = 2.67\mu_B$. IR: 2094 cm^{-1} (s, ν_{CN}).

Preparation of [V(*NS*$_3$)(MeCN)] (8a). Compound **4** (0.68 g 2.5 mmol) was refluxed in tetrahydrofuran (40 cm^3) for 2 h, cooled, and filtered into acetonitrile (10 cm^3). After 3 days the solution was taken to dryness; the residue showed IR bands characteristic of the ammine, so it was refluxed with acetonitrile for 20 min and filtered hot and the filtrate taken to dryness, giving the pure product (0.31 g, 1.1 mmol, 44%). Anal. Calcd for $C_8H_{15}N_2S_3V$: C, 33.6; H, 5.2; N, 9.8. Found: C, 33.5; H, 5.3; N, 9.9. $\mu_{eff} = 2.78\mu_B$. IR (Nujol): 2264 cm^{-1} (s, ν_{CN}).

Preparation of [V(*NS*$_3$)(Bu^{t}NC)] (8b). Compound **6** (0.68 g, 2.5 mmol) was refluxed in tetrahydrofuran (40 cm^3) for 2 h, then cooled and filtered. *tert*-Butyl isocyanide (1 cm^3) was added, giving an orange solution that was refluxed for 1 h and then filtered cold. The filtrate was reduced in vacuo to 10 cm^3, ether (10 cm^3) was added, and the brown product (0.32 g, 1.0 mmol, 40%) that precipitated was collected, washed with ether, and dried in vacuo. Anal. Calcd for $C_{11}H_{21}N_2S_3V$: C, 40.2; H, 6.4; N, 8.5. Found: C, 40.2; H, 6.5; N, 8.5. $\mu_{eff} = 2.66\mu_B$. IR (Nujol): 2173 cm^{-1} (s, ν_{NC}).

Preparation of [V(*NS*$_3$)(C$_6$H$_{11}$NC)] (8c). Compound **6** (0.68 g, 2.5 mmol) was refluxed in tetrahydrofuran (40 cm^3) and cyclohexyl isocyanide (1.0 cm^3) for 4 h. The solution was cooled and filtered. The filtrate was reduced in vacuo to 10 cm^3, ether (30 cm^3) was added, and the brown product (0.64 g, 72%) that precipitated was collected, washed with ether, and dried in vacuo. Anal. Calcd for $C_{13}H_{23}N_2S_3V$: C, 44.1; H, 6.5; N, 7.9. Found: C, 43.8; H, 6.4; N, 8.1. $\mu_{eff} = 2.74\mu_B$. IR (Nujol): 2173 cm^{-1} (s, ν_{NC}).

Preparation of [V(*NS*$_3$)(NSiMe$_3$)] (9). Compound **4** (4.44 g, 16 mmol) was suspended in a mixture of CH_3CN (160 cm^3) and trimethylsilyl azide (40 cm^3, 35 g, 0.320 mmol). The mixture was heated to reflux, and the initial yellow suspension became a dark-red solution over 3 h. It was cooled to 20 °C and filtered, leaving a small residue. The filtrate was refluxed overnight, then cooled to 20 °C and filtered, leaving no residue. The new filtrate was taken to dryness in vacuo, leaving a yellow residue that was taken up in CH_3CN (64 cm^3), refluxed for 1 h, and then filtered hot. The filtrate deposited brown-yellow crystals (suitable for X-ray study) on cooling at −20 °C overnight. Yield, 4.00 g, (12 mmol, 75%). Anal. Calcd for $C_9H_{21}N_2S_3SiV$: C, 32.5; H, 6.3; N, 8.4. Found: C, 32.9; H, 6.1; N, 8.7. ^{1}H NMR ($CDCl_3$): ∂ 0.47 (s, 9H, SiCH_3), 3.33 (m, 6H, NCH_2CH_2S), 3.65 (m, 6H, NCH_2CH_2S). ^{51}V NMR (CD_3CN): ∂ 349 (fwhm = 560 Hz).

Preparation of [V(*NS*$_3$)(NH)] (10). Compound **9** (1.33 g, 4 mmol) was suspended in methanol (20 cm^3) and acetonitrile (20 cm^3) containing four drops of water and heated to reflux. The yellow crystals quickly changed to a red powder; after 1 h the mixture was cooled at −20 °C and the resulting powdery precipitate filtered off and washed with ether (yield 0.91 g, 3.5 mmol, 88%). Crystals suitable for an X-ray study were obtained by recrystallization from acetonitrile. Anal. Calcd for $C_6H_{13}N_2S_3V$: C, 27.7; H, 5.0; N, 10.8. Found: C, 27.9; H, 5.0; N, 11.1. ^{1}H NMR ($CDCl_3$): ∂ 0.08(s, N*H*), 3.49 (m, 6H, NCH_2CH_2S), 3.71 (m, 6H, NCH_2CH_2S). ^{51}V NMR (CD_3CN): ∂ 210 (fwhm = 310 Hz). IR (Nujol): 3254 cm^{-1} (m, ν_{NH}).

Preparation of [V(*NS*$_3$)(NCPh$_3$)] (11). Trityl chloride (0.48 g, 1.67 mmol) was dried at 100 °C in vacuo for 30 min and then added to **9** (0.55 g, 1.67 mmol) in MeCN (10 cm^3). The solution was refluxed for 3 h, a red precipitate gradually forming. The mixture was then cooled, and the precipitate was filtered off, washed with ether, and dried in vacuo (0.30 g, 0.55 mmol, 33%). Anal. Calcd for $C_{25}H_{27}N_2S_3V$: C, 59.7; H, 5.4; N, 5.6. Found: C, 59.5; H, 5.4; N, 5.3. ^{1}H NMR ($CDCl_3$): ∂ 3.40 (m, 6H, NCH_2CH_2S), 3.65 (m, 6H, NCH_2CH_2S), 7.4−7.55 (m, 15H, Ph). ^{51}V NMR (CD_3CN): ∂ 234 (fwhm = 1000 Hz).

Preparation of [V(*NS*$_3$){NLi(THF)$_2$}] (12). Compound **10** (0.13 g, 0.5 mmol) was stirred in tetrahydrofuran (5 cm^3), and lithium diisopropylamide (0.3 cm^3 of 2.0 M solution, 0.6 mmol) was added, giving a yellow solution. This was filtered and ether (20 cm^3) added to the filtrate as a layer. Yellow crystals came out of solution overnight; they were filtered off, washed with ether, and dried in vacuo (0.05 g, 0.12 mmol, 24%). Anal. Calcd for $C_{14}H_{28}N_2O_2S_3LiV$: C, 41.0; H, 6.8; N, 6.8. Found: C, 40.2; H, 7.1; N, 7.1.

Preparation of [V(*NS*$_3$)(NPh)] (13a). (a) Method A. Phenyl isocyanate (2 cm^3, excess) was added to **1** (0.26 g, 1 mmol). The mixture was heated gradually to 150 °C (using a silicone oil bath) when effervescence took place, and the purple color changed to a deep red-orange. After 1 h the mixture was cooled overnight. Orange crystals formed; they were filtered off, washed with phenyl isocyanate and ether, and then dried in vacuo (0.30 g, 0.90 mmol, 90%).

(b) Method B. Aniline (2 cm^3, excess) was added to **1** (0.26 g, 1 mmol). The mixture was heated to reflux (180 °C) under a stream of dinitrogen and held at reflux for 20 min. The purple color changed to a deep red-orange. The mixture was allowed to cool and filtered cold, leaving a small residue. Diethyl ether (10 cm^3) was added as a layer to the filtrate; orange crystals formed overnight. They were filtered off, washed with diethyl ether, and dried in vacuo (0.10 g, 0.30 mmol, 30%). Anal. Calcd for $C_{12}H_{17}N_2S_3V$: C, 42.9; H, 5.1; N, 8.3. Found: C, 43.1; H, 5.0; N, 8.2. ^{1}H NMR (CD_2Cl_2): ∂ 3.43 (m, 6H, NCH_2CH_2S), 3.66 (m, 6H, NCH_2CH_2S), 7.19−7.71 (m, 5H, Ph). ^{51}V NMR (CD_3CN): ∂ 321 (fwhm = 580 Hz).

The following complexes were prepared as for **13a**, method A, above. Because some of the isocyanates are solids, 2-methoxyethyl ether (2

cm^3) was added to each preparation and reactions were carried out at the boiling point of this solvent (160 °C).

[V(*NS*$_3$)(NC$_6$H$_4$OMe-4)] (13b). Anal. Calcd for $C_{13}H_{19}N_2OS_3V$: C, 42.6; H,5.2; N, 7.7. Found: C, 42.8; H, 5.2; N,7.6. ^{1}H NMR (CD_2Cl_2): ∂ 3.40 (m, 6H, NCH_2CH_2S), 3.63, (m, 6H, NCH_2CH_2S), 3.79 (s, 3H OCH_3), 7.69 (m, 4H, Ph). ^{51}V NMR (CD_3CN): ∂ 335 (fwhm = 810 Hz).

[V(*NS*$_3$)(NC$_6$H$_4$Me-4)] (13c). Anal. Calcd for $C_{13}H_{19}N_2S_3V$: C, 44.6; H, 5.4; N, 8.0. Found: C, 46.1; H, 5.4; N, 8.1. ^{1}H NMR (C_2DCl_2): ∂ 2.45 (m, 3H CH_3), 3.50 (m, 6H, NCH_2CH_2S), 3.72 (m, 6H, NCH_2CH_2S), 7.20−7.68 (m, 4H, Ph). ^{51}V NMR (CD_3CN): ∂ 325 (fwhm = 710 Hz).

[V(*NS*$_3$)(NC$_6$H$_4$Cl-4)] (13d). Anal. Calcd for $C_{12}H_{16}ClN_2S_3V$: C, 38.9; H, 4.3; N, 7.6. Found: C, 39.2; H, 4.2; N, 7.7. ^{1}H NMR (C_2DCl_2): ∂ 3.43 (m, 6H, NCH_2CH_2S), 3.63 (m, 6H, NCH_2CH_2S), 7.30−7.65 (m, 4H, Ph). ^{51}V NMR (CD_3CN): ∂ 331 (fwhm = 890 Hz).

[V(*NS*$_3$)(NC$_6$H$_4$Br-4)] (13e). Anal. Calcd for $C_{12}H_{16}BrN_2S_3V$: C, 34.7; H, 3.9; N, 6.7. Found: C, 34.8; H, 3.8; N, 7.2. ^{1}H NMR (C_2DCl_2): ∂ 3.46 (m, 6H, NCH_2CH_2S), 3.67 (m, 6H, NCH_2CH_2S), 7.47−7.59 (m, 4H, Ph). ^{51}V NMR (CD_3CN): ∂ 331 (fwhm = 850 Hz).

[V(*NS*$_3$)(NC$_6$H$_4$NO$_2$-4)] (13f). Anal. Calcd for $C_{12}H_{16}N_3O_2S_3V$: C, 37.8; H, 4.2; N, 11.0. Found: C, 39.8; H, 4.5; N, 10.6. ^{1}H NMR (C_2DCl_2): ∂ 3.43 (m, 6H, NCH_2CH_2S), 3.63 (m, 6H, NCH_2CH_2S), 7.30−7.65 (m, 4H, Ph). ^{51}V NMR (CD_3CN): ∂ 355 (fwhm = 1500 Hz).

[V(*NS*$_3$)(NC$_6$H$_4$OMe-3)] (13 g). Anal. Calcd for $C_{13}H_{19}N_2OS_3V$: C, 42.6; H, 5.2; N, 7.7. Found: C, 42.9; H, 5.2; N, 8.2. ^{1}H NMR (CD_2Cl_2): ∂ 3.52 (m, 6H, NCH_2CH_2S), 3.73 (m, 6H, NCH_2CH_2S), 3.79 (s, 3H OCH_3), 6.86−7.41 (m, 4H, Ph). ^{51}V NMR (CD_3CN): ∂ 322 (fwhm = 760 Hz).

[V(*NS*$_3$)(NC$_6$H$_4$Cl-3)] (13h). Anal. Calcd for $C_{12}H_{16}ClN_2S_3V$: C, 38.9; H, 4.3; N, 7.6. Found: C, 38.9; H, 4.4; N, 6.9. ^{1}H NMR (CD_2Cl_2): ∂ 3.56 (m, 6H, NCH_2CH_2S). 3.76 (m, 6H, NCH_2CH_2S), 6.8−7.69 (m, 4H, Ph). ^{51}V NMR (CD_3CN): ∂ 328 (fwhm = 760 Hz).

[V(*NS*$_3$)(NC$_6$H$_3$Me$_2$-3,4)] (13i). Anal. Calcd for $C_{14}H_{21}N_2S_3V$: C, 46.2; H, 5.8; N, 7.7. Found: C, 46.5; H, 5.7; N, 8.4. ^{1}H NMR (CD_2Cl_2): ∂ 2.19 (m, 3H, CH_3), 2.28 (m, 3H, CH_3), 3.40 (m, 6H, NCH_2CH_2S), 3.63 (m, 6H, NCH_2CH_2S), 7.20−7.68 (m, 3H, Ph). ^{51}V NMR (CD_3CN): ∂ 325 (fwhm = 890 Hz).

[V(*NS*$_3$)(NC$_6$H$_3$Cl$_2$-3,4)] (13j). Anal. Calcd for $C_{12}H_{15}Cl_2N_2S_3V$: C, 35.6; H, 3.7; N, 6.9. Found: C, 35.7; H, 3.6; N, 7.3. ^{1}H NMR (CD_2Cl_2): δ 3.46 (m, 6H, NCH_2CH_2S), 3.69 (m, 6H, NCH_2CH_2S), 7.40−7.81 (m, 3H, Ph). ^{51}V NMR (CD_3CN): ∂ 337 (fwhm = 710 Hz).

[V(*NS*$_3$)(NC$_6$H$_{11}$)] 13k. Anal. Calcd for $C_{12}H_{23}N_2S_3V$: C, 42.1; H, 6.7; N, 8.2. Found: C, 43.4; H, 6.7; N,7.9. ^{1}H NMR (CD_2Cl_2): ∂ 1.88−2.24 (m, 11H, C_6H_{11}), 3.42 (m, 6H, NCH_2CH_2S), 3.62 (m, 6H, NCH_2CH_2S). ^{51}V NMR (CD_3CN): ∂ 194 (fwhm = 730 Hz).

Synthesis of [V(*OS*$_2$)O(dipp)] (14). To a hexane solution (30 cm^3) of O(CH_2CH_2SH)$_2$ (0.58 g, 4.24 mmol) and HOC$_6$H$_3$Pr$^i_2$-2,6 (0.76 g, 4.24 mmol) at room temperature was added [VO(OPr^i)$_3$], and the mixture was stirred for 10 min. The color changed to orange-red. Next, the solvent was removed in vacuo, the resulting oily residue was redissolved in CH_3CN (10 cm^3) and filtered, and the filtrate was left at 4 °C for 4 days. The resulting dark-red cubic-shaped crystals suitable for X-ray structure determination were collected by filtration, washed with cold hexane (4 °C), and dried in vacuo (82%). Anal. Calcd for $C_{16}H_{25}O_3S_2V$: C, 50.5; H, 6.6; S, 16.9. Found: C, 49.9; H, 6.5; S, 16.3. IR (Nujol): 982 cm^{-1} (s, ν_{VO}). ^{1}H NMR ($CDCl_3$): ∂ 1.18 [6H CH(CH_3)$_2$, *J* 6.8 Hz], 3.19 [1H, C*H*(CH$_3$)$_2$), *J* 6.8 Hz], 3.79 (SC*H*), 3.87 (SC*H*′), 4.08 (OC*H*), 4.68 (OC*H*′), 6.96(4-Ph), 7.00(3-Ph). ^{13}C NMR ($CDCl_3$): ∂ 23.0 [CH(*C*H$_3$)$_2$], 26.2 [*C*H(CH$_3$)$_2$], 35.4 (S*C*H), 72.8 (O*C*H), 123.7(4-Ph), 122.7(3-Ph), 135.0 (2-Ph), 165.0 (OPh). ^{51}V NMR (CD_3CN): ∂ 191.0 (fwhm = 58 Hz).

Synthesis of [V(OS$_2$)O(NNMe$_2$)(dipp)] (15). (a) Method A. To a solution of compound **14** (0.91 g, 2.39 mmol) in CH_3CN (30 cm^3) was added NH_2NMe_2 (0.58 g, 9.57 mmol), and the reaction mixture was stirred for 24 h. Next, the solvent was stripped off under vacuum to remove any excess of NH_2NMe_2. The residue was extracted with CH_3CN (20 cm^3), and the extract was filtered. The filtrate was left to crystallize at 4 °C for 3 days. Dark-red cubic-shaped crystals suitable for X-ray structure determination were collected by filtration, washed with cold hexane (4 °C), and dried in vacuo (55%). Anal. Calcd for $C_{18}H_{31}N_2O_2S_2V$: C, 51.2; H, 7.4; N, 6.7; S, 15.2. Found: C, 51.0; H, 7.3; N, 6.5; S, 15.2. ^{1}H NMR ($CDCl_3$): ∂ 1.12 [6H CH(CH_3)$_2$, *J* 6.8 Hz], 3.20 [1H, C*H*(CH$_3$)$_2$, *J* 6.8 Hz], 3.01 [6H N(CH_3)$_2$], 3.46 (SCH_2), 4.14 (OC*H*), 4.60 (OC*H*′), 6.82(4-Ph), 6.95(3-Ph). ^{13}C NMR ($CDCl_3$): ∂ 23.4 [CH(*C*H$_3$)$_2$], 26.2 [*C*H(CH$_3$)$_2$], 32.2 (S*C*H), 43.8 (N*C*H), 74.5 (O*C*H), 120.9 (4-Ph), 122.3(3-Ph), 135.2 (2-Ph), 165.1 (OPh). ^{51}V NMR (CD_3CN): ∂ 269 (fwhm = 630 Hz).

(b) Method B. The use of $Me_3SiNHNMe_2$ instead of NH_2NMe_2 and following the procedure described in method A gave compound **15**. It was identified by elemental analysis, IR, ^{1}H NMR, and the crystal cell parameters (see below).

Synthesis of [V(OS$_2$)O(NSiMe$_3$)(dipp)] (16). A mixture of compound **14** (0.5 g, 1.31 mmol) and (Me$_3$Si)$_2$NH (0.84 g, 5.25 mmol) in CH_3CN (50 cm^3) was heated under reflux for 12 h followed by stirring for a further 12 h at room temperature. The red-orange solution was filtered, and the solvent was removed in vacuo. The brown oily residue was extracted with hexane (60 cm^3), and then the extract was concentrated to half the volume and left to crystallize at room temperature. After 1 week, light-orange prismatic-shaped crystals suitable for X-ray structure determination were filtered off and dried under vacuum (20%). Anal. Calcd for $C_{19}H_{34}NO_2S_2SiV$: C, 50.5; H, 7.6; N, 3.1; S, 14.2. Found: C, 49.8; H, 7.3; N, 3.0; S, 14.6. ^{1}H NMR ($CDCl_3$): ∂ 0.04 [9H, NSi(CH_3)$_3$], 1.15 [6H CH(CH_3)$_2$, *J* 6.8 Hz], 3.25 [1H, C*H*(CH$_3$)$_2$, *J* 6.8 Hz], 3.60 (SC*H*), 3.61 (SC*H*′), 4.07 (OC*H*), 4.55 (OC*H*′), 6.87(4-Ph), 6.97(3-Ph). ^{13}C NMR ($CDCl_3$): ∂ 0.5 [NSi(*C*H$_3$)$_2$], 23.1 [CH(*C*H$_3$)$_2$], 26.2 [*C*H(CH$_3$)$_2$, 33.3 (S*C*H), 72.8 (O*C*H), 121.9 (4-Ph), 122.9(3-Ph), 134.0 (2-Ph), 166.0 (OPh). ^{51}V NMR (CD_3CN): ∂ 61 (fwhm = 365 Hz).

Synthesis of [V(OS$_2$)$_{1.5}$O] (17). To a hexane solution (30 cm^3) of O(CH_2CH_2SH)$_2$ (0.88 g, 6.36 mmol) was added [VO(OPr^i)$_3$] (1.035 g, 4.24 mmol), and the mixture was stirred for 12 h at room temperature. The resulting olive-yellow solid precipitate was filtered off, washed with hexane (3 × 10 cm^3), and dried in vacuo (87%). Anal. Calcd for $C_6H_{12}O_{2.5}S_3V$: C, 26.57; H, 4.46; S, 35.45. Found: C, 26.00; H, 4.21; S, 34.95. Compound **17** is diamagnetic.

Synthesis of [V(OS$_2$)(NNMe$_2$)(OSiMe$_3$)] (18). A mixture of compound **17** (0.21 g, 1.03 mmol) and $Me_3SiNHNMe_2$ (0.55 g, 4.15 mmol) in CH_3CN (20 cm^3) was stirred for 24 h at room temperature, and then the solvent was stripped off to remove volatile products. The residue was redissolved in CH_3CN (20 cm^3) and filtered, and the filtrate, after concentration to 10 cm^3, was left to crystallize at 4 °C for 2 days. Burgundy, X-ray-quality crystals precipitated, which were filtered, washed with cold hexane (4 °C) (3 × 2 cm^3), and dried in vacuo (80%). Anal. Calcd for $C_9H_{23}N_2O_2S_2SiV$: C, 32.3; H, 6.9; N, 8.4; S, 19.2. Found: C, 31.8; H, 6.4; N, 8.0; S, 20.1. ^{1}H NMR ($CDCl_3$): ∂ 0.08 [9H, OSi(CH_3)$_2$], 3.28 (SC*H*, *J* 5.6), 3.55 [N(CH_3)$_2$], 3.91 (OC*H*, *J* 5.6, 9.3), 4.41 (OC*H*′, *J* 5.6, 9.3). ^{13}C NMR ($CDCl_3$): ∂ 2.4 [OSi-(*C*H$_3$)$_2$], 31.7 (S*C*H$_2$), 44.9 [N(*C*H$_3$)$_2$], 74.2 (O*C*H). ^{51}V NMR (CD_3CN): ∂ 254 (fwhm = 530 Hz).

Quantitative Study of Preparation of Compound 4. Compound **1** (0.5 mmol), anhydrous hydrazine (4.88 mmol), and THF (10 cm^3) were degassed and sealed under vacuum in a glass vessel equipped with a break seal. The mixture was stirred for 3 h at 20 °C, giving a pale yellow-green solution and a yellow solid residue. The vessel was then cooled to −196 °C and opened at the break seal, and the evolved gas was pumped into a calibrated system by means of a Töpler pump and shown to be N_2 by mass spectrometry (0.22 mmol). The solution was then warmed, and the volatile NH_3 and N_2H_4 were first distilled into H_2SO_4. Then this solution was distilled from KOH solution in an all-glass apparatus into H_2SO_4. The NH_3 and N_2H_4 content of this solution (negligible and 4.10 mmol, respectively) was then determined by standard color tests.[34,35] The yellow solid was filtered off and shown to be **4** (IR spectrum identical to an authentic sample) (0.49 mmol). The remaining reaction solution was also taken to dryness in a vacuum and, after distillation from base and color tests as above, shown to contain no further NH_3 or N_2H_4.Thus, the total yield of recovered dinitrogen was 4.81 mmol (98.5% recovery) and the overall stoichiometry of the reaction was in accord with the reaction sequence, 1a → 1b → 1c of Scheme 1.

Thermal Decomposition/Disproportionation of [V(*NS*$_3$)(NH$_2$NH$_2$)] (4). Compound **4** (0.495 mmol, containing 0.99 mol N) was sealed under vacuum at −196 °C with THF (20 cm^3) and MeOH (5 cm^3) in

a glass vessel equipped with a break-seal. The mixture was heated for 1 h at 75 °C, giving a green solution and a green solid residue. The evolved gas was collected and shown to be N_2 by mass spectrometry (0.144 mmol, 0.288 mol N). The solution was then warmed, and the volatile NH_3 and N_2H_4 were determined (0.572 mmol, 0.572 mol N, and negligble, respectively). The remaining reaction solution was also taken to dryness in a vacuum and shown to have contained further NH_3 (0.096 mmol, 0.096 mol N). Thus, the total yield of recovered nitrogen was 0.956 mol N (96.5% yield based on **4**), and the overall stoichiometry of the reaction was in accord with reactions 2 and 3 above occurring consecutively.

Study of Reaction of 4 with [NEt$_4$]Cl. Compound **4** (0.53 mmol), [NEt$_4$]Cl·H$_2$O (~1 mmol), and MeCN were sealed under vacuum in an all-glass vessel equipped with a break-seal and stirred for 1 h at 20 °C. Workup as for the thermal decomposition reaction above gave compound **7a** (0.41 mmol, 78%), NH_3 (0.06 mmol), and N_2H_4 (0.51 mmol, 96%). Thus, the reaction proceeds according to eq 6 above, essentially quantitatively.

Attempted Reduction of Compound 4. Compound **4** (0.25 mmol), dipp (5 mmol), and amalgamated zinc (2.5 mmol) were sealed in a 100 cm^3 flask under argon via a septum. Then THF (10 cm^3) was added via a syringe and the mixture stirred for 72 h. Next H_2SO_4 (10 cm^3 of 0.5 M solution) was injected, and after the mixture was stirred, an excess of concentrated NaOH solution was added. The mixture was distilled into dilute H_2SO_4 and the resulting solution tested for ammonia as described above, giving 0.042 mmol NH_3, which was close to values obtained from blank runs without **4** being present. Repeating the reaction at 66 °C for 1 h gave NH_3 (0.34 mmol). This yield (due to the disproportionation reaction of **4** described above) was the same as that obtained from blanks without Zn/dipp added.

Attempted Reduction of Hydrazide Complexes. We attempted to protonate the hydrazide ligands in compounds **2b** and **2c** with halogen acid and to reduce them with Zn/HOC$_6$H$_3$Pr$^i_2$-2,6 (Hdipp) using conditions similar to those tried with **4** above, but neither protonation nor reduction was observed.

Conversion of Complex 10 into Complex 1. Compound **10** (0.5 mmol), MeOH (10 cm^3), and [NMe$_4$]OH (1 mmol) were heated at reflux for 5 min. The resulting red solution was cooled and filtered, and HCl (0.5 mmol) in Et$_2$O (0.5 cm^3) was added to give an immediate purple precipitate, which was filtered off, dried in vacuo, and identified as **1** by its IR spectrum (0.06 g, 45%).

Crystal Structure Analyses. The X-ray analyses were performed in laboratories at both the John Innes Centre and University of Wroclaw. Typical procedures from each laboratory are described, together with exceptional features in some other analyses, and all experimental data are collated in Tables 2 and 3.

Crystals of [V(*NS*$_3$)(NH$_3$)], complex **6**, are yellow, translucent plates. One, ca 0.40 mm × 0.08 mm × 0.05 mm, was mounted on a glass fiber. After preliminary photographic examination, this was transferred to an Enraf-Nonius CAD4 diffractometer (with monochromated radiation) for determination of accurate cell parameters (from the settings of 25 reflections, $\theta = 10-11°$, each centered in four orientations) and for measurement of diffraction intensities (1175 unique reflections to $\theta_{max} = 25°$; 729 were "observed" with $I > 2\sigma_I$). Subsequently, measurements of five reflections were considered suspect, and these reflections were removed from the data set.

During processing, corrections were applied for Lorentz polarization effects and absorption (by semiempirical ψ scan methods) and to eliminate negative net intensities (by Bayesian statistical methods). A small deterioration correction was also applied. The structure was determined by the automated Patterson routines in the SHELXS program[42] and refined by full-matrix least-squares methods, on F^2's, in SHELXL.[43] There is disorder in the *NS*$_3$ ligand, with the occupancy ratio of the major component to its mirror image component of ca 4:1; the thermal parameters of the major component atoms were refined anisotropically, those in the minor component isotropically. Hydrogen atoms were included on this ligand in both components, in geometrically calculated positions, with isotropic temperature factors riding on the U_{eq} or U_{iso} values of the parent carbon atoms. In the ammine ligand, hydrogen atoms were located in difference Fourier maps and included in the refinement process with geometrical constraints. Calculation of the Flack parameter both for the results quoted and for the inverse structure indicated that for the crystal chosen the absolute structure is correct. At the conclusion of the refinement, $wR_2 = 0.093$ and $R_1 = 0.085$[43] for the 1170 reflections weighted $w = \sigma^{-2}(F_o^2)$; for the "observed" data only, $R_1 = 0.049$.

In the final difference map, the highest peaks (ca 0.35 e Å^{-3}) were close to the ammine nitrogen atom.

Scattering factors for neutral atoms were taken from ref 44. Computer programs used in this analysis have been noted above or in Table 4 of ref 45 and were run on a DEC AlphaStation 200 4/100 in the Nitrogen Fixation Laboratory, John Innes Centre.

[V(*NS*$_3$)(NNMe$_2$)], complex **2b**, crystallizes as red, rectangular prisms. One was sealed in a glass capillary under a dinitrogen stream, then mounted on a KUMA KM-4 four-circle diffractometer (with monochromated Mo Kα radiation)[46] for determination of accurate cell parameters (from the settings of 25 reflections, $\theta = 8.5-13°$, each centered in four orientations) and for measurement of diffraction intensities (1218 unique reflections to $\theta_{max} = 25°$; 1118 were "observed" with $I > 2\sigma_I$).

Corrections were applied for Lorentz polarization effects; no correction for crystal deterioration was necessary. The structure was determined by direct methods in SHELXS[42] and refined by full-matrix least-squares methods, on F^2's, in SHELXL.[43] The carbon-bonded hydrogen atoms were included in calculated positions and refined using a riding model. An absorption correction, using DIFABS4,[47] was tried but gave no significant differences and so was rejected. At convergence, R_1 and wR_2 were 0.032 and 0.087 for the 1118 "observed" data weighted $w = [\sigma^2(F_o^2) + (0.046P)^2 + 0.56P]^{-1}$ with $P = (F_o^2 + 2F_c^2)/3$. In the final difference map, the highest peaks were ca 0.36 e Å^{-3} and were in the thiolate ligand.

Many crystals from several preparations of [V(*NS*$_3$)(N$_2$H$_4$)], complex **4**, were examined. Preliminary photographs showed all the samples to be multiple crystals and to have alternate sharp and "blurry" festoons on Weissenberg photographs. Eventually, a twinned crystal, with a major and minor component, with relatively little "blurriness", was found and transferred to the diffractometer. By use of the composite cell of both twins in the crystal, which looked satisfactory at least for the lower layers, intensities were measured and corrected as usual, and the structure was detemined readily by direct methods showing two independent molecules (of the major twin) in the asymmetric unit. After some refinement, examination of the major difference peaks showed the corresponding pair of molecules of the minor twin. Non-hydrogen atoms of the major twin were refined anisotropically with hydrogen atoms included in the *NS*$_3$ ligand, all parameters riding on those of the parent carbons. The minor twin was refined with some constrained bond dimensions, and only the V and S atoms allowed anisotropic thermal parameters. Refinement of the four molecules and their occupation ratio, 0.816(6):0.184, gave remarkably good results, with good agreement in the dimensions between the major molecules and with those of similar molecules (see Table 1). The *R* factors are not as low as we would normally like to present, but we believe that the structure is reliable. Further analysis of the twinning, we suggest, would not give significantly better results, since the "blurriness" along the festoons of reflections would still yield inadequacies in the measurement of diffraction intensities.

(NEt$_4$)[V(*NS*$_3$)Cl], complex **7a**, is isostructural with the iron analogue[11] and shows the same patterns of disorder in both cation and anion. The *NS*$_3$ anion lies disordered about a mirror plane, with several atoms lying in the plane and some of the ligand atoms lying on one side or the other of that plane. The cation is disordered in two major

(42) Sheldrick, G. M. *Acta Crystallogr.* **1990**, *A46*, 467.
(43) Sheldrick, G. M. SHELXL—Program for crystal structure refinement, University of Göttingen, 1993.
(44) *International Tables for X-ray Crystallography*; Kluwer Academic Publishers: Dordrecht, 1992; Vol. C, pp 500, 219, and 193.
(45) Anderson, S. N.; Richards, R. L.; Hughes, D. L. *J. Chem. Soc., Dalton Trans.* **1986**, 245.
(46) *Kuma KM-4*, version 6.1; Kuma Diffraction: Wroclaw, Poland, 1996.
(47) Walker, N.; Stuart, D. *Acta Crystallogr.* **1983**, *A39*, 158.

and two minor orientations about a 2-fold symmetry axis; site occupancies of the β-carbon atoms, after refinement, range from 0.06 to 0.5. Hydrogen atoms in the anion were included in idealized positions, and their isotropic temperature factors were allowed to refine freely. In the cation, difference peaks at ca 1.9 Å from the central nitrogen atom were included as hydrogen atoms with full site occupancy (assumed to be coincidence of atoms from molecules in several orientations) with all positional and thermal parameters refining freely. The non-hydrogen atoms of the anion, and the nitrogen atom of the cation, were refined anisotropically.

Crystals of [V(NS_3)($NSiMe_3$)], complex **9**, were analyzed independently in both laboratories; data from both are presented here as structures **1** and **2** and are seen to be very similar.

Acknowledgment. We thank the British Council, the Polish State Committee for Scientific Research, and the BBSRC for support. We also thank Dr. S. A. Fairhurst for NMR spectroscopic measurements.

Supporting Information Available: Tables listing fractional coordinates, anisotropic thermal parameters, hydrogen atom parameters, bond lengths, and bond angles. Additional data are also available in CIF format. This material is available free of charge via the Internet at http://pubs.acs.org.

IC9909476